Non-invasive reporter gene imaging of cell therapies, including T-cells and stem cells

Candice Ashmore-Harris[1,2], Madeleine Iafrate[1^], Adeel Saleem[1,3,4^], Gilbert O. Fruhwirth[1,*].

[1]Imaging Therapy and Cancer Group, Department of Imaging Chemistry and Biology, School of Biomedical Engineering and Imaging Sciences, King's College London, SE1 7EH, London, UK.

[2]Centre for Stem Cells and Regenerative Medicine, School of Basic and Medical Biosciences, King's College London, SE1 9RT, London, UK

[3]Peter Gorer Department of Immunobiology, School of Immunology and Microbial Sciences, King's College London, SE1 9RT, London, UK

[4]Department of Haematological Medicine, King's College Hospital, SE5 9RS, London, UK

^ contributed equally.

***Correspondence** should be addressed to G.O.F. (gilbert.fruhwirth@kcl.ac.uk)

Corresponding author address:
Dr Gilbert Fruhwirth, Department of Imaging Chemistry and Biology, School of Biomedical Engineering and Imaging Sciences, King's College London, St. Thomas' Hospital, Lambeth Wing 4th floor, Westminster Bridge Road SE1 7EH, London, United Kingdom. Phone: +44 20 7188 8370.
E-mail: gilbert.fruhwirth@kcl.ac.uk

Short title: Non-invasive long-term cell therapy imaging

Keywords:

adoptive cell therapy; cell tracking; immunotherapy; molecular imaging; prostate-specific membrane antigen; sodium iodide symporter.

Abstract

Cell therapies represent a rapidly emerging class of new therapeutics. They are intended and developed for the treatment of some of the most prevalent human diseases including cancer, diabetes and for regenerative medicine. Currently, they are largely developed without precise assessment of their *in vivo* distribution, efficacy or survival either clinically or preclinically. However, it would be highly beneficial for both preclinical cell therapy development and subsequent clinical use to assess these parameters *in situ* to enable enhancements in efficacy, applicability, and safety. Molecular imaging can be exploited to track cells non-invasively on the whole-body level and can enable monitoring for prolonged periods in a manner compatible with rapidly expanding cell types.

In this review, we explain how *in vivo* imaging can aid the development and clinical translation of cell-based therapeutics. We describe the underlying principles governing non-invasive *in vivo* long-term cell tracking in the preclinical and clinical settings including available imaging technologies, reporter genes and ~~contrast~~imaging agents as well as pitfalls related to experimental design. Our emphasis is on adoptively transferred T-cell and stem cell therapies.

1 Introduction

Cell-based therapy, or cell therapy, is defined as the administration of live cell products with the intention of providing effector cells to treat disease or support other treatments. Cell therapies use either cells isolated from the patient (autologous) or those from a donor (allogeneic). The type of therapeutic cell used varies widely, with clinical trials currently dominated by haematopoietic cells, mesenchymal signalling cells [1] and lymphocytes, but also, at a lesser frequency, dendritic cells, hepatocytes, epithelial cells with various others also under investigation [2, 3]. While cell therapy currently attracts much attention across various fields, it is not a new concept. In 1931, the Swiss medic P. Niehans injected fresh calf parathyroid gland cells into a human female whose own parathyroid gland had been accidentally removed during surgery; she recovered from the procedure. He claimed that embryonic animal cells would be able to regenerate human cells and organs. After more experimentation with foetal cells from black mountain sheep that were apparently resistant to cancer and other diseases, he further claimed that his fresh cell approach could help to cure cancer. However, there was a lack of scientific evidence supporting these claims and the American Cancer Society warned against unproven fresh cell therapies [4]. Allogeneic haematopoietic stem cell transplantation (HSCT) was pioneered by E.D. Thomas [5] to treat leukaemia patients, and it evolved to become the standard of care for haematological malignancies and congenital or acquired disorders of the haematopoietic system; it is also a therapeutic option in some solid tumours [6]. Oncology is currently the field responsible for over half of all cell therapy trials [2], and there have been several product approvals in recent years [7-10]. Unlike other treatments, cell therapies are live cell products and, via genetic engineering, can be enhanced to achieve better efficacy, or be tailored to benefit individual patients. The first clinically approved genetically engineered cell therapies were the chimeric antigen receptor T cell (CAR-T) therapies tisagenlecleucel and axicabtagene ciloleucel, both of which are autologous CD19-targeted CAR-T immunotherapies for the treatment of certain haematological malignancies (B-cell lymphomas; [11]). Although spectacular treatment successes have been reported for CAR-T, not all patients respond in this way, and some effects are only temporary [7, 9, 12]; additionally, CAR-T has so far generally been disappointing in solid tumours.

All cell therapies require extensive characterisation to demonstrate safety and compatibility. It is noteworthy that their *in vivo* distribution, survival and efficacy at on-target, but also off-target tissues are critical parameters. During clinical trials, off-target activities have led to severe adverse events with fatalities and other life-threatening side effects reported [13, 14]. Furthermore, most clinical cell

therapy trials are still performed without knowledge about the *in vivo* distribution and fate of the administered therapeutic cells, has resulted in suggestions to implement *in vivo* cell tracking [15-17] and suicide genes [18] into these genetically engineered cell therapies. Genetic engineering to implement additional payloads (*e.g.* reporter genes for imaging, suicide genes etc) into immune cell therapies such as CAR-Ts is less of a regulatory concern compared to genetic engineering of stem cell therapies, given that CAR-expression is enabled by genetic engineering and CAR-Ts are widely used in the clinic. In contrast, the clinical use of genetically modified stem cell therapies is not yet widespread [19, 20]. With both types of therapy, there remain several unknowns including the *in vivo* distribution, persistence and survival of cells as well as their efficacy at target and non-target sites. Consequently, broader and better investigations into these unknowns during cell therapy development and clinical translation is needed.

2 Principles of non-invasive *in vivo* cell tracking

Depending on the cell therapy being developed, traditional approaches for verifying cell survival *in vivo* relied on methods such as qPCR-based evaluations of cell retention, drug dose escalation and tumorigenicity tests. The use of molecular imaging permits the acquisition of spatiotemporal whole-body images, meaning that non-invasive *in vivo* tracking of administered therapeutic cells is now possible [21]. Cell tracking enables the quantitative assessment of several crucial aspects for cell therapy development: (i) the whole-body distribution of therapeutic cells over time; (ii) whether therapeutic cells migrate beyond the transplant site during treatment, and if so, the kinetics of this process; (iii) whether on-target bystander effects occur; and (iv) how long therapeutic cells survive. Notably, cell tracking is based on repeat-imaging of the same subjects, and therefore provides better statistical data through reduced inter-subject variability when compared to conventional approaches which relied on sacrificing animal cohorts at different time points.

2.1 Signal formation for *in vivo* cell tracking

Cell therapies cannot ordinarily be tracked in real-time, non-invasively *in vivo* by an imaging technology, without first labelling them. The labelling agent is chosen to match the desired imaging modality (*e.g.* ultrasound imaging), and it generates a detectable signal in order to provide a noticeable difference between the labelled cells and their surrounding environment. That said, the intrinsic features of some cell types of interest can be exploited to generate trackable signals. For example, when cancer cells express molecules that show low or no expression in other tissues conventional molecular imaging offers cell tracking possibilities both preclinically and clinically. As an example, using radiopharmaceutical-based molecular imaging, metastatic cells can be tracked via the sodium iodide symporter (NIS) from the thyroid [22, 23], via the glutamate carboxypeptidase 2 (prostate-specific membrane antigen/PSMA) from prostate cancer [24, 25], via the carcinoembryonic antigen (CEA) from colorectal cancers [26], or imaging melanogenic melanomas and their spread [27].

In most *in vivo* tracking scenarios, cell labels must be introduced to the cells of interest via one of two different methodologies: either direct or indirect cell labelling. Direct cell labelling is performed upon cells *ex vivo*, and the labelled cells are subsequently administered to subjects for cell tracking using the relevant imaging technology (Fig.1A). Uptake of the labelling agent can be achieved by exploiting normal cellular processes (*e.g.* through phagocytosis, via internalizing receptors etc.) or assisted (*e.g.* by transfection agents or coupling of the contrast agent to membrane translocation peptides). A wide

variety of ready-to-use contrast agents that are compatible with all relevant imaging technologies are available [21]. Conversely, indirect labelling requires cells to be genetically engineered to ectopically express a reporter gene, rendering them different from the surrounding cells *in vivo* (Fig.1B). The reporter is normally integrated permanently into cells (see Section 2.2) and it must allow them to be targeted by molecular imaging *in vivo* following administration of a suitable labelling agent. Therefore, the relatively simple process of molecular imaging can be performed repeatedly (whereas the cell labelling only needs to occur once), allowing the genetically modified cells to be tracked longitudinally.

There are three principal strategies that ensure reporter genes afford indirectly labelled cells detectable signal for *in vivo* imaging. These rely on the reporter gene coding for either an enzyme, cell surface protein or transport protein (Fig.1C). Where the reporter gene yields expression of a functional enzyme it is catalysis of the administered substrate that renders the cells trackable, *e.g.* through entrapment of the signal within reporter expressing cells (*e.g.* the radiolabelled substrates of HSV1-*tk*, tyrosinase) or the generation of a signal (*e.g.* luciferases converting a chemical into detectable light). Cell surface protein~~s~~-based reporter genes exploit binding of a labelling agents for imaging (*e.g.* receptor binding a labelled ligand). It is noteworthy that some reporter proteins have enzymatic capacity but the latter is not utilised for imaging (e.g. PSMA and its variants [28, 29] or estrogen receptor [30]). Transporter protein reporters enable a labelled substrate to be transferred into cells to generate a signal. All these mechanisms can be useful for preclinical cell tracking. However, for clinical cell tracking, the emphasis lies on cell surface proteins, transporters and enzymes entrapping molecular probes (Fig.1C/1-3), because signal-generating proteins (Fig.1C/4) are often either not of human origin (*e.g.* luciferase) or produce potentially toxic products if expressed outside their endogenous niche (*e.g.* tyrosinase; [31]). A notable exception are certain mammalian nucleoside kinases [32]. Alongside improvements in imaging technologies, corresponding reporter gene-afforded cell labelling agents have been developed and optimised. Reporter genes can either be foreign in relation to the host organism or represent self; according to these criteria several promising reporter genes are listed in Tab.1 and Tab.2.

2.2 Gene transfer methods for reporter gene introduction

Traditionally, genetic engineering has been achieved through the use of viral vectors (*e.g.* γ-retroviruses, lentiviruses), which more or less randomly integrate the transgenes into the genome [33]. This approach is often also classified as 'gene therapy' and has been applied for cell therapies in diverse aetiologies ranging from cancer immunotherapies to the regulation of immune tolerance in

autoimmune diseases [14]. Lentiviruses are capable of efficiently transducing both actively dividing and non-dividing cell types, making them particularly valuable for stable gene transfer to mature somatic cells and lineage-committed, non-proliferating cells (*i.e.* differentiated from stem cells). In contrast, γ-retroviruses efficiently transduce only actively dividing cells, and have been commercially approved for use in gene therapy applications for *ex vivo* modification of T-cells and haematopoietic stem cells [34]. In some cases,. Random genomic integration is associated with the risk of alterating normal gene function at or around the integration site. Moreover, effects on the inserted reporter cannot be ruled out as well as epigenetic silencing. To mitigate this episomal plasmids have also been used, which can yield stable transgene expression (*e.g.* when delivered by transfection or electroporation; [35, 36]). Gene editing, a form of genetic engineering, offers a much more specific way of integrating a desired genetic payload at a distinct location into the genome of target cells [37, 38]. The latter might be. Provided a suitable integration site is selected this can enable stable reporter gene expression even in instances where there is high proliferation. This is of particular utility in the context of stem cell therapies, where random integration of therapeutic, reporter and suicide genes would pose risks of both insertional mutagenesis and downstream silencing. In fact, gene editing is already in use clinically for a range of cell therapies due to these inherent advantages [20].

3 Experimental design considerations for indirect cell tracking

Planning reporter gene-afforded (indirect) *in vivo* cell tracking experiments requires careful consideration of diverse parameters such as: whether the study is staged in a preclinical or clinical setting, whether immunocompetent or immunocompromised host organisms will be used, the type of imaging technology, desired therapeutic cell detection sensitivity, overall observation period and desired imaging intervals, and labelling agent availability.

3.1 Cell detection sensitivity

Exquisite detection sensitivity is required for *in vivo* cell tracking. It is dictated by both the choice of reporter gene and its corresponding contrast agent as well as the matched imaging technology.

Firstly, the reporter-signal pair must be detected by a matching imaging technology. Ideally, it should offer molecular sensitivities in, or below, the picomolar concentration range (Fig.2). The most suitable imaging technologies are therefore bioluminescence and radionuclide modalities; only in special cases can other imaging technologies fare as well for *in vivo* cell tracking. For example, tracking of melanin-producing murine melanoma cell spread was achieved in mice at reasonable sensitivity and

resolution compared to the study goals by using photoacoustic tomography [39]. Importantly, many disease models require 3D tomographic imaging in rodents or larger mammals, *i.e.* non-translucent organisms. Consequently, optical imaging technologies are unfavourable due to their inherent limitations relating to light scattering and absorption by tissues. While extremely sensitive, bioluminescence cannot provide accurate and reliable 3D information. Hence, radionuclide imaging modalities are generally preferable for *in vivo* cell tracking from this perspective.

Secondly, cell detection sensitivity depends on reporter expression levels and the molecular imaging mechanism underlying its targeting by the ~~contrast~~imaging agent (Fig.1C). Transporters (*e.g.* NIS or NET) provide signal amplification as each reporter protein can transport several radiotracer molecules into the cell. Taking NIS as an example, its endogenous expression is highest in thyroid cells, whereas ectopic expression as a transgenic reporter protein in non-thyroidal cells occurs within a mechanistically distinct environment. In these circumstances, iodide radiotracers are not metabolised into thyroid hormones [22], and consequently radioiodide is subject to different cell residence times and efflux kinetics. NIS is also promiscuous in anion selection for uptake, which has enabled the development of iodine-free single photon emission computed tomography (SPECT) and positron emission tomography (PET) tracers, such as $^{99m}TcO_4^-$ (SPECT), $[^{18}F]BF_4^-$, $[^{18}F]SO_3^-$, or $[^{18}F]PF_6^-$ (PET) having recently been reported as alternatives with proof-of-principle shown in animal models [40-43]. These benefit from better decay properties and avoid the drawbacks of undergoing cellular entrapment and metabolization in the thyroid, relative to earlier radioiodide tracers. Reporters which enzymatically entrap radiotracers that are taken up into cells by different mechanisms also offer high cell detection sensitivities due to ~~contrast agent~~molecular probe accumulation. Examples include the cytosolic thymidine and cytidine kinases (Tab.1-2), which irreversibly phosphorylate the radiotracers when inside (mammalian) cells, thus preventing the radiotracers from being transported back out of the cells. A potential drawback is that these kinases could potentially shift the relevant biochemical equilibria in cells as they also accept the natural substrates; this could alter cell metabolism, however, systematic studies investigating this aspect are currently not available. Non-enzymatic cell surface molecules such as receptors tend to be less sensitively detected, because they form one-to-one complexes ~~with~~when bound to their ~~contrast agent binders~~molecular probes. Moreover, they can get internalised upon ligand binding, which then impacts detection sensitivity through reduction of their steady-state concentration on the plasma membrane (*e.g.* human somatostatin receptor 2 (SSTR2);[44]). Importantly, the molecular imaging mechanisms should not be regarded in isolation, and other aspects, for example endogenous reporter expression or corresponding probe excretion

properties, are additional crucial aspects to achieve good target-to-background rations (see examples in Section 4).

The detection sensitivities of NIS-expressing extra-thyroidal cells have been reported preclinically to be as good as hundreds/thousands for cancer cells expressing NIS *in vitro* [45, 46], and CAR-Ts expressing PSMA *in vitro* and *in vivo* [29], or tens of thousands for effector T-cells using various different reporter genes *in vivo* [47]. Notably, the human norepinephrine transporter (NET) was found to most sensitively detect reporter-expressing T-cells in a direct reporter comparison study between various nucleoside kinases and the transporters NIS and NET [47]; however, the endogenous NET expression and background signals generally obtained by NET imaging are not favourable for T-cell tracking (Tab.1). As reporter expression levels are cell type-dependent, it is advisable to determine their sensitivities on existing instrumentation.

3.2 Resolution

Currently, the imaging methodologies providing best sensitivities are not at the forefront in terms of resolution, providing only millimetre resolution. An exception is fixed-collimator SPECT instrumentation, which has been reported to offer preclinical resolutions of 0.25 mm [48], albeit at rather long image acquisition times. In contrast, exquisite resolution is offered by computed tomography (CT) and magnetic resonance imaging (MRI), but neither are suitable for generating sufficient contrast in reporter gene-afforded cell tracking at present. The strengths of both have been exploited through combination imaging approaches with highly sensitive radionuclide and bioluminescence technologies, a concept termed multi-modal imaging [49, 50]. In multi-modal imaging, the higher resolution anatomical images complement the high sensitivity images, and the resultant combined images thus enable detected signals to be more readily attributed to their anatomical context when reconstructed. For *in vivo* cell tracking, multi-modal imaging is now the norm with SPECT/CT, PET/CT, PET/MRI and bioluminescence/CT routinely used preclinically and both PET/CT and PET/MRI advantageous in the clinical setting.

3.3 Observation time and interval

Reporter gene-afforded cell tracking is superior to direct cell-labelling methods in terms of observation time as it does not suffer from label dilution effects or depend on long-term contrast agent presence (and thus is not affected by contrast agent efflux) (Fig.1A-B). This renders reporter gene methods particularly suitable for tracking cells longitudinally, and for tracking rapidly dividing cells (*e.g.*

expanding T-lymphocyte-derived therapies, teratomas), as the reporter gene is inherited by progeny cells, giving rise to theoretically indefinite observation times. In practice, observation times are limited by cell survival and the limit of detection (as traceable cells could become so widely distributed at low concentrations that they fall below the limit of detection).

The principle of reporter gene imaging rests on the attribution of imaging signals to the cells expressing the reporter protein (Fig1B-C). The labelling agent used for this application depends on the chosen imaging modality. Focussing on nuclear imaging techniques that provide high sensitivity and are prime for translation to clinical use (as explained in Section 3.2), the radiotracer must emit photons at a rate that allows detection by SPECT or PET. The rate at which nuclear material emits photons, or decays, defines its half-life; generally, the physical half-life (τ) of the radionuclide chosen should match the half-life of the biological process that will be imaged (for example, the time taken for a radiotracer to penetrate tissues and accumulate in cells). For theoretically indefinite cell tracking, one would need to use a radiotracer with a theoretically indefinite half-life – this is obviously impractical for imaging and for the patient! However, with reporter gene technology, it is now possible to achieve this goal by repeated administration of short-lived (*i.e.* minutes/hours) radioisotopes, such as ^{18}F (τ = 1.8 h). The choice of radionuclide is of paramount importance. It is important to choose a reporter gene-signal-pair offering optimal repeat imaging intervals (Tab.1). For example, there are various radiotracers available for thymidine kinase reporters, including [^{18}F]FEAU, [^{123}I]FIAU, or [^{124}I]FIAU. They have distinct radioisotopes incorporated with differing half-lives, *i.e.* ^{18}F (τ = 1.8 h), $^{123}I^-$ (τ = 13.2 h) or $^{124}I^-$ (τ = 4.2 d). With current instrumentation, between four and five half-lives are required for radiotracers to sufficiently decay to undetectable levels for a low enough background signal to permit subsequent imaging sessions (~6% radiotracer left assuming the worst-case scenario of no excretion) [46]. On the other hand, radiotracers with very short half-lives are not advantageous, as they could lead to sub-optimal reporter detection (if the radiotracer has a relatively longer circulation time) or make experiments logistically challenging, requiring multiple radiotracer productions on the same day. Therefore, radiotracers with half-lives in the low hour-range, for example ^{18}F or ^{99m}Tc, appear to be a good compromise for experimental designs requiring imaging intervals of ~days. Whilst repeat imaging adds experimental complexity when using radionuclide techniques, as the tracer must be prepared for each imaging session (Fig.1B), the short-lived radiotracers offer the additional advantage that cells receive significantly lower doses of radiation compared to using direct cell labelling methods over the same tracking period.

3.4 Cell viability and its impact on detected cell tracking signals

Indirect cell tracking using reporter genes is fundamentally linked to cell viability, as only viable cells translate the reporter protein, a process that requires cellular energy. The differing molecular imaging mechanisms (Fig.1C) of different reporter proteins also impact how rapidly changes in cell viability can be detected. First, every reporter protein is subject to production and degradation within the respective cellular environment. These processes are naturally unique to each reporter, and it should be noted that cell biological turnover parameters are poorly understood for most reporters employed for *in vivo* cell tracking. The exceptions are fluorescent proteins, which due to their extensive use in cell biology, have been thoroughly investigated in this respect [51]. There are even fluorescent protein variants reported that change their fluorescence spectrum as a function of the time passed since production, so-called fluorescent timers [52, 53]. Other groups have manipulated the turnover kinetics of fluorescent proteins through genetic modification or linked it to distinct cellular events. An example of the latter is the fusion of an oxygen-dependent degradation domain (ODD) to a fluorescent protein; this resulted in rapid fluorescent protein turnover under normoxia but stabilisation of the reporter when cells underwent hypoxia [54]. This approach building on the ODD from the hypoxia-inducible factor 1α is generally suitable for cytosolic proteins, and its applicability was earlier demonstrated for a luciferase reporter [55]. However, a caveat of using fluorescent and bioluminescent reporters in hypoxic conditions is that their signal generation is reliant on the presence of oxygen, especially luciferase [56], and this impacts upon the quantification of hypoxia, likely underestimating true signals. Interestingly, this was also found to be true for thymidine kinases but not for the β-galactosidase reporter [56], albeit the latter plays no role for *in vivo* cell tracking. This means that reporter function can depend on the environment in the cell, and potentially can also be exploited to report on distinct cellular conditions.

When interrogating cell viability, it is also worth noting that receptor/membrane-protein-based reporters only require binding of the signal/label. This may lead to the detection of fragmented reporter protein, cell debris, or dying yet still traceable cells, at least until clearance of debris by the organism. Transporter reporter genes overcome this issue, because they require a cellular gradient spanning the plasma membrane of an intact cell. For example, NIS requires an intact Na^+ gradient for uptake of radiolabelled anions, which is upheld by cellular Na^+/K^+ ATPase [57], an enzyme requiring ATP for function. Once the Na^+ gradient cannot be upheld, *e.g.* through loss of cellular energy or perforation of cell membranes, NIS-mediated transport is compromised and radiotracer signals for imaging are no

longer accumulated in cells. In studies tracking cancer cells, this phenomenon was observed by authors reporting images with tumour cores free of NIS signals, demonstrating that dead and dying cancer cells in the necrotic tumour core were not detected, in line with mechanistic expectations [45, 58, 59]. This means that transporters report cell viability in a more direct manner, being sensitive to cellular energy depletion and death faster than reporters relying solely on protein presence.

3.5 Host-compatible reporters *versus* foreign reporters

The host immune status is a major design parameter for all reporter gene imaging applications, as it is fundamentally intertwined with reporter gene selection and the achievable contrast throughout the body. For optimal contrast, a foreign reporter that is expressed nowhere in the host organism would be favourable, as there would be zero background reporter gene expression and therefore no background signal (colloquially referred to as "noise"). Such foreign reporters are, for instance, fluorescent proteins, luciferases [60] or the PET reporter herpes simplex virus 1 thymidine kinase (HSV1-*tk*) [61-63]. However, the *in vivo* distribution of the labelling agent can cause a level of noise. Whilst this can be avoided with enzyme-activated signals such as those emanating from the luciferase/luciferin reporter/label pair, the situation is different when using radiolabelled agents, since radioactive decay is a physical property that cannot be modulated, activated, or terminated. Consequently, signals detected as a result of radioactive decay must only be interpreted once the radiolabel has had the proper time to circulate, become distributed according to their molecular specificity, and be eliminated from other tissues (Fig.3). In practice, this means that even foreign radionuclide imaging reporters are not totally free of background signals; however, unlike bioluminescence, they enable quantitative 3D imaging (Fig.2). Foreign reporter genes have been shown to function in numerous preclinical cell tracking studies, performed most frequently in heavily immunocompromised animal models.

Where the host organism is immunocompetent or only partly immunocompromised, immunogenicity of the reporter becomes a major experimental design determinant. Any foreign protein, and consequently any cells presenting it (*e.g.* via major histocompatibility complexes (MHC) class I or II), can elicit an immune response (Fig.4). Ultimately, the expression of a foreign reporter molecule can cause the destruction of the administered therapeutic cells by the immune system (Fig.4). Consequently, host-compatible reporters have received considerable attention. These are reporter genes that are from the same species as the host but are endogenously expressed in only a very limited number of host tissues, and ideally at low levels to ensure favourable contrast in adjacent organs (Fig.3). Obviously, the selected host-compatible reporter should not be expressed in organs of interest

for the intended cell tracking study, as this would detrimentally impact the detectability of traceable cells.

4 Cell tracking in T-cell therapy development

Alongside the emergence of anti-cancer immunotherapies, including adoptively transferred T-cell immunotherapies, it became necessary to develop methods to image T-cells *in vivo*. T-cell-specific properties were exploited for this, including cell surface molecules unique to T-cells (markers) or specific to particular T-cell subsets. Detection of T-cells has focused on antibodies or antibody fragments directed against these markers and conjugated to suitable labelling agents (predominantly radioisotopes for high-sensitivity imaging). Examples include: targeting the T-cell receptor (TCR; *e.g.* [64, 65]), the T-cell surface glycoprotein cluster of differentiation 3 (CD3; [66]), the Helper T-cell marker CD4, as well as the Cytotoxic T-cell marker CD8 [67-69]. A general limitation to this approach is that the obtained imaging signals cannot be used to back-calculate T-cell numbers because the precise expression levels of T-cell surface marker molecules are unknown at the point of imaging. As for adoptively transferred T-cell immunotherapies, an additional limitation of imaging T-cells with molecular probes is the lack of discrimination between the therapeutic cells and host T-cells. While the cited examples probe T-cell presence, the same limitations exist for methods probing T-cell activation.

To overcome this, the adoptively transferred cells were labelled to distinguish them from the resident ones, using both direct and indirect cell labelling approaches, where the general considerations for reporter gene imaging apply. Moreover, T-cells are relatively sensitive to radiation-induced damage compared to other cell types (*cf.* animal irradiation is a routine method to ablate cells of the immune system), hence reporter gene methods which expose labelled cells to lower radiation doses for long-term tracking are even more favourable. Various reporter genes have been used for tracking adoptively transferred T-cells. Early studies employed the HSV1-*tk* as a reporter gene and demonstrated excellent contrast due to its foreign nature and good sensitivity across the range of its corresponding PET radiotracers (Tab.2; Fig.5A). To assess T-cell activation, an inducible reporter exploiting the nuclear factor of transcription (NFAT) binding sites for regulation of reporter expression was described [70]. Inducible reporter genes are becoming an important element in the quest to drive reporter gene imaging beyond conventional cell tracking and toward reporting therapeutic activity. To appropriately quantify signal changes, it is best to normalise to an intrinsic constitutive signal, or beacon, which is provided

by a second reporter. This concept has been demonstrated repeatedly *in vitro* across various research fields by co-expression using different reporters, for example in oncology and immunology [71-74]. Recently, a transgenic mouse has been reported that utilises two foreign reporters: one luciferase which serves as an NFAT-driven T-cell activation marker, and another spectrally different luciferase which operates as a beacon for normalisation of T-cell signals [73]. HSV1-*tk* has also been chosen for the first proof-of-principle study of reporter gene imaging in humans. This was performed in heavily pre-treated interleukin-13 receptor α2-positive recurrent glioblastoma patients whose prognosis was generally poor [75]; they received $CD8^+$ cytotoxic T-lymphocytes (CTL) engineered to express both the interleukin-13 zetakine chimeric antigen receptor and the reporter [76]. While the CTL tracking was found to be successful, the cohort size was too small to link CTL trafficking and viability to clinical outcome. The above studies were performed in immunocompromised animal hosts and heavily pre-treated late-stage cancer patients, respectively, and therefore the documented immunogenicity of HSV1-*tk* [77] has not been a major concern. However, for the development and potential future *in vivo* monitoring of T-cell therapies, host-compatible reporters are necessary.

Various host reporters (Fig.4, centre left) have been developed, utilising clinically approved ~~contrast~~imaging agents that were already available (Tab.1). Human SSTR2 has shown some potential for cell tracking based on the existence of clinically approved PET tracers (*e.g.* [^{68}Ga]Ga-DOTATATE (antagonist) or [^{68}Ga]Ga-DOTATOC (agonist)), and has been used preclinically for CAR-T tracking [78, 79]. However, a significant pitfall of using SSTR2 as a reporter is that it is endogenously expressed in various tissues including the kidneys and gastrointestinal tract [80] and, importantly, on a variety of immune cell types (T-cells, B-cells and macrophages; [81]), which negatively affects imaging specificity in immunocompetent models, and likely humans. Furthermore, it was found that the agonist impaired immune function in humans [82]. During imaging radiotracer concentrations are generally very low, but it cannot be ruled out without further study that somatostatin analogues and its ~~contrast~~imaging agent derivatives do not impair some immune functions. Another important caveat of the SSTR2 reporter is that it internalises upon ligand binding [44, 83], thus potentially negatively impacting detection sensitivity (*cf.* Section 3.1). Mammalian NIS has been used in a variety of cell tracking applications in animal models spanning a wide range of different cell types [45, 84-92]. This is a testament to both its excellent contrast in many applications, as NIS is only endogenously expressed in the thyroid and a few extra-thyroidal tissues (salivary glands, mammary glands, stomach and small intestine, testes; [22]), and its small anionic radiotracers being readily available for both PET and SPECT imaging (Tab.1). Notably, if NIS is used together with non-iodine radiotracers such as

393 [^{18}F]BF_4^-, signal-to-background is favourable compared to iodide tracers [46]. Recently, NIS has also
394 been exploited in preclinical models for CAR-T cell therapy tracking, focussed on trafficking to
395 prostate cancer and breast cancer models [93, 94]. Prostate-specific membrane antigen (PSMA) has
396 also been developed as a reporter gene [28], mainly due to its extremely limited endogenous expression
397 and the fact that several clinically approved radiotracers for imaging are available, which were
398 originally intended for molecular imaging of PSMA-expressing prostate cancers and their metastases
399 [95]. Interaction of PSMA with its ligand can also result in its internalisation [95, 96], which is sensitive
400 to certain amino acid modifications at the N-terminus of PSMA [97]. For its use as a reporter gene, a
401 PSMA variant was designed to prevent its internalization and increase its surface expression while also
402 lacking the putative intracellular signalling motifs. This engineered tPSMA^{N9Del} variant has been used
403 to track CAR-T cells in an acute lymphoblastic leukaemia model by PET using an ^{18}F-radiolabelled
404 version of its high-affinity ligand DCFPyL [29]. Interestingly, the authors reported that CAR-T signals
405 obtained from tumours did not correlate with easily accessible peripheral CAR-T blood counts or CAR-
406 T presence in the bone marrow, demonstrating the importance of spatiotemporal cell therapy imaging
407 for accurate monitoring of CAR-T trafficking (Fig.5C).

408 Another route to reporters with low immunogenicity and good contrast features is to generate
409 artificial proteins consisting of host proteins or their domains. To achieve targeting of these chimeras,
410 incorporation of antibody fragments as extracellular domains that can be targeted with corresponding
411 labelling agents have been reported. For example, murine and human monovalent anti-polyethylene
412 glycol (PEG) fragments without Fc portions have been developed as reporter genes with corresponding
413 labelling agents based on PEG conjugated to a range of diverse labelling agents (^{124}I for PET,
414 superparamagnetic iron oxide nanoparticles for MRI and a near-infrared fluorophore for optical
415 imaging) [98]. These approaches were benchmarked for imaging specificity relative to HSV1-*tk* and
416 similar results were seen. However, they have yet to be tested in T-cells. In a similar approach, a single-
417 chain fragment (scFv) of the murine anti-lanthanoid-DOTA (1,4,7,10-tetraazacyclododecane-1,4,7,10-
418 tetraacetic acid) IgG1 antibody 2D12.5/G54C [99, 100] was fused with a human IgG4-CH2-CH3
419 spacer and the transmembrane domain of human CD4 (DAbR1). The scFv was found to bind
420 irreversibly to yttrium-(*S*)-2-(4-acrylamidobenzyl-)-DOTA (AABD), which could serve as an imaging
421 label when conjugated to an appropriate radioisotope (*e.g.* using ^{86}Y for PET imaging). DAbR1 was
422 successfully expressed on lymphocytes and CD19 CAR T-cells. To detect the traceable cells,
423 radiotracer was administered 30 minutes after T-cell injection, with subsequent PET detection showing
424 good contrast 16h (~1.1 half-lives) [101]. While offering a high positron yield, a limitation for

longitudinal T-cell reporter gene imaging with ^{86}Y is its long half-life (τ = 14.7h) which only permits re-imaging after about three days (*cf.* Section 3.3). Its long positron range also impacts resolution (comparable to ^{124}I and about two-fold worse resolution than that of the gold standard, ^{18}F [102]). These studies demonstrate potentially workable approaches, but are still in preliminary stages, as none of the reporter genes are fully human/humanised. It remains to be seen if fully humanised chimeras will become available for T-cell imaging. A step ahead in this respect is a reporter gene incorporating the human carcino-embryonic antigen (hCEA) fused to one of various validated human cell surface protein domains to anchor it within the plasma membrane [103, 104]. In this case, an antibody or antibody fragment is required to detect hCEA, which is almost exclusively expressed in certain cancers. While tracking agents can be built on the corresponding antibodies/antibody fragments and the whole system is fully human, it is still unsuitable for adoptive T-cell therapy tracking if the corresponding cancer or cancer model also expresses hCEA.

Notably, adoptive T-cell therapies have been hampered by severe side-effects [13, 14]. *In vivo* cell tracking offers the significant advantage to detect mis-targeting, *i.e.* unsafe conditions. Imaging of therapeutic mistargeting is dependent on the level of signal at the unintended site, and therefore varies depending on the disease model, the therapy targeting moieties and the employed reporter gene. A one-size-fits-all approach to detect mistargeting at different anatomical locations may be feasible with a foreign reporter (providing there are favourable excretion properties of the corresponding radiotracer) but this would be limited to use in only immunocompromised/immunodeficient disease models. To advance the development of adoptive T-cell therapies in syngeneic models, and ultimately for monitoring therapies in patients, the development of host reporters is necessary. Moreover, host reporter gene selection needs to be tailored to the model/condition and the target. Only *in vivo* cell tracking will be able to measure and inform spatiotemporally on therapeutic cell targeting and mistargeting. This requires truly quantitative longitudinal imaging to accurately, reliably and reproducibly quantify signals from administered cells and background, thus better implementation of unbiased physical and mathematical analysis methods will need to be used to advance this in the future. Ultimately, these approaches will unlock the ability to intervene earlier in the event of therapeutic mistargeting and thereby avoid the detrimental effects at the off-target site. This intervention could involve utilising so-called 'suicide genes'. Some host reporters could be repurposed to act as suicide genes if radiotracers are modified appropriately from labelling/signal generation agent to radiotherapeutic using matched-pair radioisotopes, thus ablating the cell therapy (*e.g.* NIS: $^{131}I^-$ or $^{188}ReO_4^-$; PSMA: ^{177}Lu-PSMA-ligand etc.). However, these approaches tend to be slow in their killing

response and potentially also induce radiation damage in bystander cells. Instead, dedicated suicide genes have been developed for cell and gene therapies. This includes the inducible caspase-9 (iCaspase9) which is activatable by a cell-permeable dimeriser drug and results in ablation of suicide gene expressing cells. iCaspase9 shows rapid function (>90% within 30min; [105]) even in the brain [106], which is crucial in emergency cases. Its main disadvantage is dimeriser drug availability. Thus, alternative approaches have been developed including: RQR8 (combined target epitopes from CD34 and CD20 antigens), which binds the widely used pharmaceutical antibody rituximab resulting in selective deletion of transgene-expressing cells [107]; a ligand binding and kinase-dead EGFR variant targetable with the pharmaceutical antibody cetuximab [108]; and a rapamycin-activatable iCaspase9 [109]. While the latter is suitable for anti-cancer CAR-T, it is not suitable for cell therapies relying on rapamycin for their production, *e.g.* regulatory T-cell therapies [110-112]. Both RQR8 and iCaspase9 are already in clinical trials (NCT02808442, NCT02746952, NCT02735083, NCT03939026, NCT03190278, NCT04106076, NCT04142619 and NCT03721068, NCT02849886, NCT04180059). Nevertheless, the full potential of suicide genes, which enable early destruction of mis-targeted therapeutic cells before severe clinical signs become evident, has yet to be fulfilled. This may be achieved in the future by combining detection of early indicators of mistargeting with *in vivo* tracking and quantification of administered cell therapies.

5 Cell tracking in stem cell therapy development

5.1 Clinical tracking of stem cell therapies

Numerically, so-called ‘mesenchymal stem cells’ make up the highest number of stem cell therapies used in clinical trials to date, although strictly speaking these are often not *bona fide* stem cell therapies and are more accurately described as a heterogeneous population of multipotent mesenchymal signalling/stromal cells (MSCs), which may contain stem cell subpopulations [1]. In fact, hundreds of clinical trials using these variously defined MSC populations have been performed to date [1, 113]. However, in spite of their regenerative potential, MSCs tend to have poor levels of engraftment upon transplant, and it is now believed that their value as cell therapies are to promote self-healing of the damaged tissues through the release of cytokines, chemokines and growth factors which, in turn, offer the capacity to promote native tissue regeneration and recruit or activate cells at the injury site that encourage regeneration. This contrasts with other therapies using stem/progenitor

cells (SCs) or their differentiated progeny, where the goal is to achieve high levels of engraftment post-transplant and often also differentiation, or maturation of the transplanted SC population within its niche. As such, transient cell survival would be a limiting factor to therapeutic benefit. Consequently, it is now recognised that the ability to monitor cells post-transplant via non-invasive *in vivo* tracking could hold the key to improving cell survival and engraftment.

Despite the many potential benefits, only a handful of SC therapy studies utilising *in vivo* imaging have been performed in the clinic. To our knowledge, these have all adopted a direct cell labelling approach using either MRI or PET/SPECT modalities to track transplanted cell fate. Autologous neural SCs, mesenchymal signalling/stromal cells and haematopoietic SCs have all been directly labelled (Fig.1A), and then monitored *in vivo* to assess: neuroregeneration for both trauma injuries and neurodegenerative diseases [114, 115], anti-fibrotic therapeutic effects in advanced liver cirrhosis [116], or cardiac repair [117-119]. Given the regulatory hurdles associated with genetic engineering of stem cells, avoidance of reporter gene imaging approaches for tracking SC therapies clinically is unsurprising.

5.2 Reporter gene afforded pre-clinical tracking of stem cell therapies

Comparatively, in the preclinical arena, the potential for reporter genes to enable tracking of SCs isolated from adult tissues, pluripotent SCs (PSCs) such as human embryonic SCs (hESCs) and human induced PSCs (hiPSCs), as well as PSC-differentiated progeny *in vivo* is gaining interest. In Tab.3 we list studies using preclinical reporter gene-afforded *in vivo* imaging of SC populations (or their *in vitro* differentiated progeny) of human origin. Notably, numerous imaging studies using SC populations derived from a range of animal sources have also been reported (e.g [90, 120, 121]). While some reports demonstrate tracking of SC populations isolated from adult tissues, the bulk of studies have focused on developing tools to monitor tumourigenicity of hESCs and hiPSCs *in vivo* or to enable monitoring of survival and engraftment of PSC differentiated progeny. In the case of tumourigenicity, studies monitoring PSC survival and teratoma formation are vital for providing safety assurances prior to use in humans. Undifferentiated PSCs possess tumourigenic potential, so longitudinal *in vivo* imaging allows transplanted differentiated cell populations to be monitored for residual, contaminating PSCs. If PSCs are present in only low numbers, tumour formation may take time to yield a palpable tumour or may be present in deep tissue or at off-target sites, so the nature of monitoring required is incompatible with direct cell labelling approaches. Reporter gene imaging, however, can offer cell

tracking over longer time-frames, and the possibility to determine the minimum number of PSCs that would go on to form a tumour, allowing differentiation purity thresholds to be set [122, 123] (Fig.6).

For cell populations differentiated from PSCs, aside from monitoring tumourigenicity, the goal of *in vivo* imaging is typically to assess engraftment and survival post-transplant. Whilst direct cell labelling can inform on immediate survival post-transplant, reporter gene imaging is again needed to assess the long-term survival of these therapies. At the preclinical level such monitoring can aid in important therapeutic decisions such as site of transplant (ectopic site or within appropriate tissue niche), required cell numbers to enable longitudinal cell survival, level of engraftment and whether factors such as transplantation of organoids, cell scaffolds, or use of a supporting extracellular matrix would be necessary, all whilst using appropriate animal models for the intended patient population.

Whilst PSC-derived therapies are costly to produce, they have already entered early clinical trials [124], and as their use for treating a greater range of injuries and diseases comes ever closer to clinical reality, reporter gene studies become increasingly important. Most early PSC therapy tracking studies incorporated the reporter cassette via lentiviral transduction and utilised the firefly luciferase (fLuc) reporter gene to enable BLI, often with an additional reporter co-expressed for streamlining preclinical experimentation, *e.g.* a fluorescent protein to simplify cell generation (Tab.3). Use of BLI is due to its exquisite sensitivity at low running and investment cost, despite sacrificing 3D information for 2D-projected images. BLI has been shown to address narrow questions relating to graft survival adequately. Assessment of therapy relocalisation *in vivo* is also feasible by BLI, albeit at the expense of identification of the off-target site, as BLI does not provide true 3D tomographic information. Radionuclide reporter gene imaging could help overcome this limitation, but it has been employed only by a few studies using human PSCs to date [92, 123, 125, 126]. Additionally, while studies using lentiviral-mediated reporter expression have mostly demonstrated stable reporter expression following both differentiation and PSC expansion, the risk of epigenetic silencing and viral integration at unwanted genomic sites remains. Consequently, gene editing as a means for incorporation of transgenes into safe harbour loci has been widely employed for *in vitro* research [127]. While initially focused on fluorescent proteins and microscopy, this approach is now emerging for *in vivo* imaging-compatible reporter genes including those required for cell tracking by BLI and radionuclide imaging. Exploiting the adeno-associated virus integration site 1 (AAVS1) locus and using zinc finger nucleases (ZFNs) for stable reporter gene expression has been observed in both hESCs and differentiated cells [128, 129].

A final point to consider is that of the studies tracking hESCs there has been a significant focus on use of the earliest lines derived at the University of Wisconsin, *i.e.* H1, H7, H9 [130]. Whilst easily commercially available, like hiPSCs, these lines have widely been reported to be prone to acquiring significant genomic abnormalities following extended periods of propagation, dependent on culture conditions [131]. Unlike hESCs though, systematically characterised allogeneic hiPSC banks are in production across the globe, to enable high levels of immunocompatibility with the population ahead of wider clinical application of regenerative medicines, thus hiPSC tracking studies may prove to be the most translationally relevant stem cell tracking technology moving forward [13~~1~~2].

Field Code Changed

6 Considerations for clinical application or reporter gene imaging and outlook

Cell therapies can be classified as either (a) not in need of genetic engineering for efficacy (*e.g.* all currently approved stem cell therapies, tumour infiltrating lymphocytes, γδ T-cells etc.), or (b) fundamentally requiring genetic engineering for efficacy (*e.g.* CAR-T, TCR-T). For *in vivo* tracking of the first group, the choice between direct and indirect cell labelling depends on the precise research question, practicalities, and of course whether clinical translation of the tracking methodology is envisaged and for what purpose. Implementing genetic engineering for the sole purpose of clinical long-term cell tracking currently appears out of reach for these therapies as it adds a significant regulatory burden and potential risk depending on the gene transfer technique used, all of which is difficult to justify. Consequently, recently developed direct cell tracking approaches (*e.g.* based on [^{89}Zr]Zr-oxine and matched with PET imaging [133-135]) are promising tools despite their obvious limitations caused by the cell labelling methodology itself (label efflux, label dilution, complex dosimetry, limited observation times). The situation is likely to improve through the development of total-body PET, which has been reported to be 40-times more sensitive than conventional PET [136]. This sensitivity advantage could either be invested into faster PET scanning, scanning with reduced radioactivity, or both of the above. Future *in vivo* cell tracking studies using total-body PET technology will reveal to what extent this sensitivity advantage can be used to extend the tracking time of directly labelled cells.

For cell-based immunotherapies that require genetic engineering, an immunocompatible host reporter gene can be implemented without adding to the regulatory burden. Indirect cell labelling is clearly advantageous over direct cell labelling in such cases as it enables longer-term monitoring,

reflects cell proliferation and viability, and avoids complex dosimetry considerations during cell labelling. Precise radiobiological characterisation of the effects of radiotracer uptake and decay within immune cells and stem cells has not yet been fully elucidated. However, the use of short-lived radioisotopes, particularly for PET-afforded reporter gene imaging, provides a clear dose reduction compared to any form of long-term cell tracking using direct radioisotope labelling approaches. Genetic engineering technologies have steadily advanced and include viral and non-viral delivery methods as well as site-specific integration via gene editing approaches (Fig.3C). While new vectors inherently trigger safety evaluations and thus are expensive to develop, there has still been significant progress in this domain in recent years [137, 138], with ready-to-use platforms for clinical use available [7, 12]. Crucially, reporter genes must be co-delivered either in the same or a separate vector with therapeutic genes, for example the CAR. This has previously been demonstrated by rendering CAR-Ts traceable by SPECT or PET [29, 94] and is fundamentally the same concept as is exploited for adding other therapy-relevant payloads such as CAR-dependent expression of immune checkpoint antibodies or cytokines (*cf.* different CAR-T generations and armoured CARs; [139]). If activity of therapeutic cells is envisaged, a system with two reports, an inducible one and a beacon reporter can be employed, which in principle could also operate for radionuclide reporters. However, in the context of clinical translation, such an approach would add a high level of complexity, duplicating effort, cost, and likely resulting in logistically more convoluted reporter gene imaging. This is because it would require concurrent supply of two radiotracers which can either be discriminated temporally through different administration/imaging time windows or discriminated by simultaneous dual-isotope imaging approaches (*e.g.* afforded by SPECT or dual-isotope PET [140-142]). Currently, such methods are not routinely available either preclinically or clinically. More research is needed to devise new smart reporter systems compatible with radionuclide imaging which can also report on environmental changes, for example CAR T-cell activity, without the need for a second reporter for normalisation. Another crucial aspect for clinical reporter gene imaging is the range of suitable labelling agents available. A scenario where labelling agents are already clinically approved, non-toxic and widely and easily accessible (*e.g.* radiotracers such as $^{99m}TcO_4^-$ and $[^{18}F]BF_4^-$ for NIS or [^{68}Ga]Ga-PSMA-ligands for PSMA) is obviously advantageous compared to the development of a reporter gene that would additionally require lengthy radiopharmaceutical development and subsequent regulatory approval. It is unlikely that a one-size-fits-all approach across varying cell therapies and disease conditions will be ever available in the future. For example, in oncology cancers differ in their anatomical location, hence involving only one immunocompatible host reporter gene/radiotracer pair for cell therapy tracking is very unlikely to meet all requirements. More likely, various cancers at different anatomical sites with

varying endogenous host reporter expression levels will be targeted by genetically engineered cell-based immunotherapies, where the target as well as the host reporter will be somewhat tailored to the individual patient.

All of the above concepts can be extrapolated to cell therapies intended to treat other conditions, such as those in the fields of regenerative medicine [143], transplantation [111, 144], diabetes type I [145, 146], multiple sclerosis [147], and infectious diseases [148]. Undoubtedly, to drive reporter gene imaging closer to future routine clinical application, more research into optimising existing and developing new host reporter/labelling agent pairs is warranted. This will offer the most flexible toolkit to render cell therapies traceable *in vivo* with the best contrast and optimal read-out, in a truly quantitative manner.

Acknowledgments

The authors received support from Guy's & St. Thomas' Charity (PhD studentship to CAH), EPSRC and GE Healthcare (PhD studentship to MI), MRC (PhD studentship to AS) and Cancer Research UK *via* a Multidisciplinary Project Award [C48390/A21153] to GOF. Furthermore they are supported by the King's College London and UCL Comprehensive Cancer Imaging Centre, funded by Cancer Research UK and EPSRC; the National Institute for Health Research (NIHR) Biomedical Research Centre based at Guy's and St Thomas' NHS Foundation Trust and King's College London; and the Wellcome/EPSRC Centre for Medical Engineering at King's College London [WT 203148/Z/16/Z]. Institutional Open Access funds to support article publication were also received. The views expressed are those of the authors and not necessarily those of the NHS, the NIHR, or the DoH. Aspects of figures 1, 3, and 4 were created with Biorender.com.

Author Contributions

GF contributed the article concept; MI and GF compiled the figures; CAH, MI, AS and GF wrote sections of the manuscript. All authors contributed to literature searches, manuscript revision, read and approved the submitted version.

Conflict of Interest

The authors declare that the research was conducted in the absence of any commercial or financial relationships that could be construed as a potential conflict of interest.

References

1. Caplan, AI (2017). Mesenchymal Stem Cells: Time to Change the Name! *Stem Cells Transl Med* **6**: 1445-1451.
2. Heathman, TR, Nienow, AW, McCall, MJ, Coopman, K, Kara, B, and Hewitt, CJ (2015). The translation of cell-based therapies: clinical landscape and manufacturing challenges. *Regen Med* **10**: 49-64.
3. Bioinformant (2019). Bioinformant Cell Therapy Industry Database. BioInformant.
4. Society, AC (1991). Unproven methods of cancer management. Fresh cell therapy. *CA Cancer J Clin* **41**: 126-128.
5. Thomas, ED, Lochte, HL, Jr., Lu, WC, and Ferrebee, JW (1957). Intravenous infusion of bone marrow in patients receiving radiation and chemotherapy. *N Engl J Med* **257**: 491-496.
6. Appelbaum, FR (2007). Hematopoietic-cell transplantation at 50. *N Engl J Med* **357**: 1472-1475.
7. Neelapu, SS, Locke, FL, Bartlett, NL, Lekakis, LJ, Miklos, DB, Jacobson, CA, *et al.* (2017). Axicabtagene Ciloleucel CAR T-Cell Therapy in Refractory Large B-Cell Lymphoma. *N Engl J Med* **377**: 2531-2544.
8. Schuster, SJ, Bishop, MR, Tam, CS, Waller, EK, Borchmann, P, McGuirk, JP, *et al.* (2019). Tisagenlecleucel in Adult Relapsed or Refractory Diffuse Large B-Cell Lymphoma. *N Engl J Med* **380**: 45-56.
9. Schuster, SJ, Svoboda, J, Chong, EA, Nasta, SD, Mato, AR, Anak, O, *et al.* (2017). Chimeric Antigen Receptor T Cells in Refractory B-Cell Lymphomas. *N Engl J Med* **377**: 2545-2554.
10. USFood&DrugAdministration (2017). FDA approves CAR-T cell therapy to treat adults with certain types of large B-cell lymphoma. vol. 2018.
11. USFood&DrugAdministration (2017). FDA approval brings first gene therapy to the United States. vol. 2018.
12. Maude, SL, Laetsch, TW, Buechner, J, Rives, S, Boyer, M, Bittencourt, H, *et al.* (2018). Tisagenlecleucel in Children and Young Adults with B-Cell Lymphoblastic Leukemia. *N Engl J Med* **378**: 439-448.
13. Linette, GP, Stadtmauer, EA, Maus, MV, Rapoport, AP, Levine, BL, Emery, L, *et al.* (2013). Cardiovascular toxicity and titin cross-reactivity of affinity-enhanced T cells in myeloma and melanoma. *Blood* **122**: 863-871.
14. Saudemont, A, Jespers, L, and Clay, T (2018). Current Status of Gene Engineering Cell Therapeutics. *Front Immunol* **9**: 153.
15. Fruhwirth, GO, Kneilling, M, de Vries, IJM, Weigelin, B, Srinivas, M, and Aarntzen, E (2018). The Potential of In Vivo Imaging for Optimization of Molecular and Cellular Anti-cancer Immunotherapies. *Mol Imaging Biol* **20**: 696-704.
16. Krekorian, M, Fruhwirth, GO, Srinivas, M, Figdor, CG, Heskamp, S, Witney, TH, *et al.* (2019). Imaging of T-cells and their responses during anti-cancer immunotherapy. *Theranostics* **9**: 7924-7947.
17. Volpe, A, Kurtys, E, and Fruhwirth, GO (2018). Cousins at work: How combining medical with optical imaging enhances in vivo cell tracking. *Int J Biochem Cell Biol* **102**: 40-50.
18. Jones, BS, Lamb, LS, Goldman, F, and Di Stasi, A (2014). Improving the safety of cell therapy products by suicide gene transfer. *Front Pharmacol* **5**: 254.
19. Abou-El-Enein, M, Bauer, G, Reinke, P, Renner, M, and Schneider, CK (2014). A roadmap toward clinical translation of genetically-modified stem cells for treatment of HIV. *Trends Mol Med* **20**: 632-642.

20. Ashmore-Harris, C, and Fruhwirth, GO (2020). The clinical potential of gene editing as a tool to engineer cell-based therapeutics. *Clin Transl Med* **9**: 15.
21. Kircher, MF, Gambhir, SS, and Grimm, J (2011). Noninvasive cell-tracking methods. *Nat Rev Clin Oncol* **8**: 677-688.
22. Portulano, C, Paroder-Belenitsky, M, and Carrasco, N (2014). The Na+/I- symporter (NIS): mechanism and medical impact. *Endocr Rev* **35**: 106-149.
23. Kogai, T, and Brent, GA (2012). The sodium iodide symporter (NIS): regulation and approaches to targeting for cancer therapeutics. *Pharmacol Ther* **135**: 355-370.
24. Oliveira, JM, Gomes, C, Faria, DB, Vieira, TS, Silva, FA, Vale, J, *et al.* (2017). (68)Ga-prostate-specific Membrane Antigen Positron Emission Tomography/Computed Tomography for Prostate Cancer Imaging: A Narrative Literature Review. *World J Nucl Med* **16**: 3-7.
25. Perera, M, Papa, N, Christidis, D, Wetherell, D, Hofman, MS, Murphy, DG, *et al.* (2016). Sensitivity, Specificity, and Predictors of Positive (68)Ga-Prostate-specific Membrane Antigen Positron Emission Tomography in Advanced Prostate Cancer: A Systematic Review and Meta-analysis. *Eur Urol* **70**: 926-937.
26. Tiernan, JP, Perry, SL, Verghese, ET, West, NP, Yeluri, S, Jayne, DG, *et al.* (2013). Carcinoembryonic antigen is the preferred biomarker for in vivo colorectal cancer targeting. *Br J Cancer* **108**: 662-667.
27. Tsao, H, Chin, L, Garraway, LA, and Fisher, DE (2012). Melanoma: from mutations to medicine. *Genes Dev* **26**: 1131-1155.
28. Castanares, MA, Mukherjee, A, Chowdhury, WH, Liu, M, Chen, Y, Mease, RC, *et al.* (2014). Evaluation of prostate-specific membrane antigen as an imaging reporter. *J Nucl Med* **55**: 805-811.
29. Minn, I, Huss, DJ, Ahn, HH, Chinn, TM, Park, A, Jones, J, *et al.* (2019). Imaging CAR T cell therapy with PSMA-targeted positron emission tomography. *Sci Adv* **5**: eaaw5096.
30. Qin, C, Lan, X, He, J, Xia, X, Tian, Y, Pei, Z, *et al.* (2013). An in vitro and in vivo evaluation of a reporter gene/probe system hERL/(18)F-FES. *PLoS One* **8**: e61911.
31. Urabe, K, Aroca, P, Tsukamoto, K, Mascagna, D, Palumbo, A, Prota, G, *et al.* (1994). The inherent cytotoxicity of melanin precursors: a revision. *Biochim Biophys Acta* **1221**: 272-278.
32. Lee, JT, Zhang, H, Moroz, MA, Likar, Y, Shenker, L, Sumzin, N, *et al.* (2017). Comparative Analysis of Human Nucleoside Kinase-Based Reporter Systems for PET Imaging. *Mol Imaging Biol* **19**: 100-108.
33. Goswami, R, Subramanian, G, Silayeva, L, Newkirk, I, Doctor, D, Chawla, K, *et al.* (2019). Gene Therapy Leaves a Vicious Cycle. *Front Oncol* **9**: 297.
34. Ghani, K, Boivin-Welch, M, Roy, S, Dakiw-Piaceski, A, Barbier, M, Pope, E, *et al.* (2019). Generation of High-Titer Self-Inactivated gamma-Retroviral Vector Producer Cells. *Mol Ther Methods Clin Dev* **14**: 90-99.
35. Ronald, JA, Cusso, L, Chuang, HY, Yan, X, Dragulescu-Andrasi, A, and Gambhir, SS (2013). Development and validation of non-integrative, self-limited, and replicating minicircles for safe reporter gene imaging of cell-based therapies. *PLoS One* **8**: e73138.
36. Lufino, MM, Edser, PA, and Wade-Martins, R (2008). Advances in high-capacity extrachromosomal vector technology: episomal maintenance, vector delivery, and transgene expression. *Mol Ther* **16**: 1525-1538.
37. Maggio, I, and Goncalves, MA (2015). Genome editing at the crossroads of delivery, specificity, and fidelity. *Trends Biotechnol* **33**: 280-291.
38. Bressan, RB, Dewari, PS, Kalantzaki, M, Gangoso, E, Matjusaitis, M, Garcia-Diaz, C, *et al.* (2017). Efficient CRISPR/Cas9-assisted gene targeting enables rapid and precise genetic manipulation of mammalian neural stem cells. *Development* **144**: 635-648.

39. Lavaud, J, Henry, M, Coll, JL, and Josserand, V (2017). Exploration of melanoma metastases in mice brains using endogenous contrast photoacoustic imaging. *Int J Pharm* **532**: 704-709.
40. Khoshnevisan, A, Chuamsaamarkkee, K, Boudjemeline, M, Jackson, A, Smith, GE, Gee, AD, *et al.* (2017). 18F-Fluorosulfate for PET Imaging of the Sodium-Iodide Symporter: Synthesis and Biologic Evaluation In Vitro and In Vivo. *J Nucl Med* **58**: 156-161.
41. Jiang, H, Bansal, A, Goyal, R, Peng, KW, Russell, SJ, and DeGrado, TR (2018). Synthesis and evaluation of (18)F-hexafluorophosphate as a novel PET probe for imaging of sodium/iodide symporter in a murine C6-glioma tumor model. *Bioorg Med Chem* **26**: 225-231.
42. Jauregui-Osoro, M, Sunassee, K, Weeks, AJ, Berry, DJ, Paul, RL, Cleij, M, *et al.* (2010). Synthesis and biological evaluation of [(18)F]tetrafluoroborate: a PET imaging agent for thyroid disease and reporter gene imaging of the sodium/iodide symporter. *Eur J Nucl Med Mol Imaging* **37**: 2108-2116.
43. O'Doherty, J, Jauregui-Osoro, M, Brothwood, T, Szyszko, T, Marsden, PK, O'Doherty, MJ, *et al.* (2017). (18)F-Tetrafluoroborate, a PET Probe for Imaging Sodium/Iodide Symporter Expression: Whole-Body Biodistribution, Safety, and Radiation Dosimetry in Thyroid Cancer Patients. *J Nucl Med* **58**: 1666-1671.
44. Cescato, R, Schulz, S, Waser, B, Eltschinger, V, Rivier, JE, Wester, HJ, *et al.* (2006). Internalization of sst2, sst3, and sst5 receptors: effects of somatostatin agonists and antagonists. *J Nucl Med* **47**: 502-511.
45. Fruhwirth, GO, Diocou, S, Blower, PJ, Ng, T, and Mullen, GE (2014). A whole-body dual-modality radionuclide optical strategy for preclinical imaging of metastasis and heterogeneous treatment response in different microenvironments. *J Nucl Med* **55**: 686-694.
46. Diocou, S, Volpe, A, Jauregui-Osoro, M, Boudjemeline, M, Chuamsaamarkkee, K, Man, F, *et al.* (2017). [(18)F]tetrafluoroborate-PET/CT enables sensitive tumor and metastasis in vivo imaging in a sodium iodide symporter-expressing tumor model. *Sci Rep* **7**: 946.
47. Moroz, MA, Zhang, H, Lee, J, Moroz, E, Zurita, J, Shenker, L, *et al.* (2015). Comparative Analysis of T Cell Imaging with Human Nuclear Reporter Genes. *J Nucl Med* **56**: 1055-1060.
48. Ivashchenko, O, van der Have, F, Villena, JL, Groen, HC, Ramakers, RM, Weinans, HH, *et al.* (2014). Quarter-millimeter-resolution molecular mouse imaging with U-SPECT(+). *Mol Imaging* **13**.
49. Basu, S, Hess, S, Nielsen Braad, PE, Olsen, BB, Inglev, S, and Hoilund-Carlsen, PF (2014). The Basic Principles of FDG-PET/CT Imaging. *PET Clin* **9**: 355-370, v.
50. Catana, C (2017). Principles of Simultaneous PET/MR Imaging. *Magn Reson Imaging Clin N Am* **25**: 231-243.
51. Khmelinskii, A, Meurer, M, Ho, CT, Besenbeck, B, Fuller, J, Lemberg, MK, *et al.* (2016). Incomplete proteasomal degradation of green fluorescent proteins in the context of tandem fluorescent protein timers. *Mol Biol Cell* **27**: 360-370.
52. Subach, FV, Subach, OM, Gundorov, IS, Morozova, KS, Piatkevich, KD, Cuervo, AM, *et al.* (2009). Monomeric fluorescent timers that change color from blue to red report on cellular trafficking. *Nat Chem Biol* **5**: 118-126.
53. Terskikh, A, Fradkov, A, Ermakova, G, Zaraisky, A, Tan, P, Kajava, AV, *et al.* (2000). "Fluorescent timer": protein that changes color with time. *Science* **290**: 1585-1588.
54. Misra, T, Baccino-Calace, M, Meyenhofer, F, Rodriguez-Crespo, D, Akarsu, H, Armenta-Calderon, R, *et al.* (2017). A genetically encoded biosensor for visualising hypoxia responses in vivo. *Biol Open* **6**: 296-304.
55. Goldman, SJ, Chen, E, Taylor, R, Zhang, S, Petrosky, W, Reiss, M, *et al.* (2011). Use of the ODD-luciferase transgene for the non-invasive imaging of spontaneous tumors in mice. *PLoS One* **6**: e18269.

56. Cecic, I, Chan, DA, Sutphin, PD, Ray, P, Gambhir, SS, Giaccia, AJ, *et al.* (2007). Oxygen sensitivity of reporter genes: implications for preclinical imaging of tumor hypoxia. *Mol Imaging* **6**: 219-228.
57. Dohan, O, De la Vieja, A, Paroder, V, Riedel, C, Artani, M, Reed, M, *et al.* (2003). The sodium/iodide Symporter (NIS): characterization, regulation, and medical significance. *Endocr Rev* **24**: 48-77.
58. Edmonds, S, Volpe, A, Shmeeda, H, Parente-Pereira, AC, Radia, R, Baguna-Torres, J, *et al.* (2016). Exploiting the Metal-Chelating Properties of the Drug Cargo for In Vivo Positron Emission Tomography Imaging of Liposomal Nanomedicines. *ACS Nano* **10**: 10294-10307.
59. Volpe, A, Man, F, Lim, L, Khoshnevisan, A, Blower, J, Blower, PJ, *et al.* (2018). Radionuclide-fluorescence Reporter Gene Imaging to Track Tumor Progression in Rodent Tumor Models. *J Vis Exp* **133**: e57088.
60. Mezzanotte, L, van 't Root, M, Karatas, H, Goun, EA, and Lowik, C (2017). In Vivo Molecular Bioluminescence Imaging: New Tools and Applications. *Trends Biotechnol* **35**: 640-652.
61. Gambhir, SS, Bauer, E, Black, ME, Liang, Q, Kokoris, MS, Barrio, JR, *et al.* (2000). A mutant herpes simplex virus type 1 thymidine kinase reporter gene shows improved sensitivity for imaging reporter gene expression with positron emission tomography. *Proc Natl Acad Sci U S A* **97**: 2785-2790.
62. Likar, Y, Dobrenkov, K, Olszewska, M, Shenker, L, Cai, S, Hricak, H, *et al.* (2009). PET imaging of HSV1-tk mutants with acquired specificity toward pyrimidine- and acycloguanosine-based radiotracers. *Eur J Nucl Med Mol Imaging* **36**: 1273-1282.
63. Yaghoubi, SS, and Gambhir, SS (2006). PET imaging of herpes simplex virus type 1 thymidine kinase (HSV1-tk) or mutant HSV1-sr39tk reporter gene expression in mice and humans using [18F]FHBG. *Nat Protoc* **1**: 3069-3075.
64. Yusufi, N, Mall, S, Bianchi, HO, Steiger, K, Reder, S, Klar, R, *et al.* (2017). In-depth Characterization of a TCR-specific Tracer for Sensitive Detection of Tumor-directed Transgenic T Cells by Immuno-PET. *Theranostics* **7**: 2402-2416.
65. Griessinger, CM, Maurer, A, Kesenheimer, C, Kehlbach, R, Reischl, G, Ehrlichmann, W, *et al.* (2015). 64Cu antibody-targeting of the T-cell receptor and subsequent internalization enables in vivo tracking of lymphocytes by PET. *Proc Natl Acad Sci U S A* **112**: 1161-1166.
66. Larimer, BM, Wehrenberg-Klee, E, Caraballo, A, and Mahmood, U (2016). Quantitative CD3 PET Imaging Predicts Tumor Growth Response to Anti-CTLA-4 Therapy. *J Nucl Med* **57**: 1607-1611.
67. Seo, JW, Tavare, R, Mahakian, LM, Silvestrini, MT, Tam, S, Ingham, ES, *et al.* (2018). CD8(+) T-Cell Density Imaging with (64)Cu-Labeled Cys-Diabody Informs Immunotherapy Protocols. *Clin Cancer Res* **24**: 4976-4987.
68. Freise, AC, Zettlitz, KA, Salazar, FB, Lu, X, Tavare, R, and Wu, AM (2017). ImmunoPET Imaging of Murine CD4(+) T Cells Using Anti-CD4 Cys-Diabody: Effects of Protein Dose on T Cell Function and Imaging. *Mol Imaging Biol* **19**: 599-609.
69. Tavare, R, Escuin-Ordinas, H, Mok, S, McCracken, MN, Zettlitz, KA, Salazar, FB, *et al.* (2016). An Effective Immuno-PET Imaging Method to Monitor CD8-Dependent Responses to Immunotherapy. *Cancer Res* **76**: 73-82.
70. Ponomarev, V, Doubrovin, M, Lyddane, C, Beresten, T, Balatoni, J, Bornman, W, *et al.* (2001). Imaging TCR-dependent NFAT-mediated T-cell activation with positron emission tomography in vivo. *Neoplasia* **3**: 480-488.
71. Serganova, I, Cohen, IJ, Vemuri, K, Shindo, M, Maeda, M, Mane, M, *et al.* (2018). LDH-A regulates the tumor microenvironment via HIF-signaling and modulates the immune response. *PLoS One* **13**: e0203965.

72. Serganova, I, Doubrovin, M, Vider, J, Ponomarev, V, Soghomonyan, S, Beresten, T, *et al.* (2004). Molecular imaging of temporal dynamics and spatial heterogeneity of hypoxia-inducible factor-1 signal transduction activity in tumors in living mice. *Cancer Res* **64**: 6101-6108.
73. Kleinovink, JW, Mezzanotte, L, Zambito, G, Fransen, MF, Cruz, LJ, Verbeek, JS, *et al.* (2018). A Dual-Color Bioluminescence Reporter Mouse for Simultaneous in vivo Imaging of T Cell Localization and Function. *Front Immunol* **9**: 3097.
74. Mezzanotte, L, An, N, Mol, IM, Lowik, CW, and Kaijzel, EL (2014). A new multicolor bioluminescence imaging platform to investigate NF-kappaB activity and apoptosis in human breast cancer cells. *PLoS One* **9**: e85550.
75. Brown, CE, Warden, CD, Starr, R, Deng, X, Badie, B, Yuan, YC, *et al.* (2013). Glioma IL13Ralpha2 is associated with mesenchymal signature gene expression and poor patient prognosis. *PLoS One* **8**: e77769.
76. Keu, KV, Witney, TH, Yaghoubi, S, Rosenberg, J, Kurien, A, Magnusson, R, *et al.* (2017). Reporter gene imaging of targeted T cell immunotherapy in recurrent glioma. *Sci Transl Med* **9**.
77. Berger, C, Flowers, ME, Warren, EH, and Riddell, SR (2006). Analysis of transgene-specific immune responses that limit the in vivo persistence of adoptively transferred HSV-TK-modified donor T cells after allogeneic hematopoietic cell transplantation. *Blood* **107**: 2294-2302.
78. Zhang, H, Moroz, MA, Serganova, I, Ku, T, Huang, R, Vider, J, *et al.* (2011). Imaging expression of the human somatostatin receptor subtype-2 reporter gene with 68Ga-DOTATOC. *J Nucl Med* **52**: 123-131.
79. Vedvyas, Y, Shevlin, E, Zaman, M, Min, IM, Amor-Coarasa, A, Park, S, *et al.* (2016). Longitudinal PET imaging demonstrates biphasic CAR T cell responses in survivors. *JCI Insight* **1**: e90064.
80. Yamada, Y, Post, SR, Wang, K, Tager, HS, Bell, GI, and Seino, S (1992). Cloning and functional characterization of a family of human and mouse somatostatin receptors expressed in brain, gastrointestinal tract, and kidney. *Proc Natl Acad Sci U S A* **89**: 251-255.
81. Elliott, DE, Li, J, Blum, AM, Metwali, A, Patel, YC, and Weinstock, JV (1999). SSTR2A is the dominant somatostatin receptor subtype expressed by inflammatory cells, is widely expressed and directly regulates T cell IFN-gamma release. *Eur J Immunol* **29**: 2454-2463.
82. Barsegian, V, Hueben, C, Mueller, SP, Poeppel, TD, Horn, PA, Bockisch, A, *et al.* (2015). Impairment of lymphocyte function following yttrium-90 DOTATOC therapy. *Cancer Immunol Immunother* **64**: 755-764.
83. Oomen, SP, Hofland, LJ, Lamberts, SW, Lowenberg, B, and Touw, IP (2001). Internalization-defective mutants of somatostatin receptor subtype 2 exert normal signaling functions in hematopoietic cells. *FEBS Lett* **503**: 163-167.
84. Groot-Wassink, T, Aboagye, EO, Wang, Y, Lemoine, NR, Keith, WN, and Vassaux, G (2004). Noninvasive imaging of the transcriptional activities of human telomerase promoter fragments in mice. *Cancer Res* **64**: 4906-4911.
85. Sieger, S, Jiang, S, Schonsiegel, F, Eskerski, H, Kubler, W, Altmann, A, *et al.* (2003). Tumour-specific activation of the sodium/iodide symporter gene under control of the glucose transporter gene 1 promoter (GTI-1.3). *Eur J Nucl Med Mol Imaging* **30**: 748-756.
86. Merron, A, Peerlinck, I, Martin-Duque, P, Burnet, J, Quintanilla, M, Mather, S, *et al.* (2007). SPECT/CT imaging of oncolytic adenovirus propagation in tumours in vivo using the Na/I symporter as a reporter gene. *Gene Ther* **14**: 1731-1738.
87. Dingli, D, Kemp, BJ, O'Connor, MK, Morris, JC, Russell, SJ, and Lowe, VJ (2006). Combined I-124 positron emission tomography/computed tomography imaging of NIS gene

expression in animal models of stably transfected and intravenously transfected tumor. *Mol Imaging Biol* **8**: 16-23.
88. Carlson, SK, Classic, KL, Hadac, EM, Dingli, D, Bender, CE, Kemp, BJ, *et al.* (2009). Quantitative molecular imaging of viral therapy for pancreatic cancer using an engineered measles virus expressing the sodium-iodide symporter reporter gene. *AJR Am J Roentgenol* **192**: 279-287.
89. Higuchi, T, Anton, M, Saraste, A, Dumler, K, Pelisek, J, Nekolla, SG, *et al.* (2009). Reporter gene PET for monitoring survival of transplanted endothelial progenitor cells in the rat heart after pretreatment with VEGF and atorvastatin. *J Nucl Med* **50**: 1881-1886.
90. Terrovitis, J, Kwok, KF, Lautamaki, R, Engles, JM, Barth, AS, Kizana, E, *et al.* (2008). Ectopic expression of the sodium-iodide symporter enables imaging of transplanted cardiac stem cells in vivo by single-photon emission computed tomography or positron emission tomography. *J Am Coll Cardiol* **52**: 1652-1660.
91. Che, J, Doubrovin, M, Serganova, I, Ageyeva, L, Zanzonico, P, and Blasberg, R (2005). hNIS-IRES-eGFP dual reporter gene imaging. *Mol Imaging* **4**: 128-136.
92. Ashmore-Harris, C, Blackford, SJ, Grimsdell, B, Kurtys, E, Glatz, MC, Rashid, TS, *et al.* (2019). Reporter gene-engineering of human induced pluripotent stem cells during differentiation renders in vivo traceable hepatocyte-like cells accessible. *Stem Cell Res* **41**: 101599.
93. Kurtys, E, Lim, L, Man, F, Volpe, A, and Fruhwirth, G (2018). In vivo tracking of CAR-T by [18 f]BF 4 - PET/CT in human breast cancer xenografts reveals differences in CAR-T tumour retention. *Cytotherapy* **20**: S20.
94. Emami-Shahri, N, Foster, J, Kashani, R, Gazinska, P, Cook, C, Sosabowski, J, *et al.* (2018). Clinically compliant spatial and temporal imaging of chimeric antigen receptor T-cells. *Nat Commun* **9**: 1081.
95. O'Keefe, DS, Bacich, DJ, Huang, SS, and Heston, WDW (2018). A Perspective on the Evolving Story of PSMA Biology, PSMA-Based Imaging, and Endoradiotherapeutic Strategies. *J Nucl Med* **59**: 1007-1013.
96. Liu, H, Rajasekaran, AK, Moy, P, Xia, Y, Kim, S, Navarro, V, *et al.* (1998). Constitutive and antibody-induced internalization of prostate-specific membrane antigen. *Cancer Res* **58**: 4055-4060.
97. Rajasekaran, SA, Anilkumar, G, Oshima, E, Bowie, JU, Liu, H, Heston, W, *et al.* (2003). A novel cytoplasmic tail MXXXL motif mediates the internalization of prostate-specific membrane antigen. *Mol Biol Cell* **14**: 4835-4845.
98. Chuang, KH, Wang, HE, Cheng, TC, Tzou, SC, Tseng, WL, Hung, WC, *et al.* (2010). Development of a universal anti-polyethylene glycol reporter gene for noninvasive imaging of PEGylated probes. *J Nucl Med* **51**: 933-941.
99. Corneillie, TM, Whetstone, PA, Lee, KC, Wong, JP, and Meares, CF (2004). Converting weak binders into infinite binders. *Bioconjug Chem* **15**: 1389-1391.
100. Goodwin, DA, Meares, CF, Watanabe, N, McTigue, M, Chaovapong, W, Ransone, CM, *et al.* (1994). Pharmacokinetics of pretargeted monoclonal antibody 2D12.5 and 88Y-Janus-2-(p-nitrobenzyl)-1,4,7,10-tetraazacyclododecanetetraacetic acid (DOTA) in BALB/c mice with KHJJ mouse adenocarcinoma: a model for 90Y radioimmunotherapy. *Cancer Res* **54**: 5937-5946.
101. Wei, LH, Olafsen, T, Radu, C, Hildebrandt, IJ, McCoy, MR, Phelps, ME, *et al.* (2008). Engineered antibody fragments with infinite affinity as reporter genes for PET imaging. *J Nucl Med* **49**: 1828-1835.
102. Lubberink, M, and Herzog, H (2011). Quantitative imaging of 124I and 86Y with PET. *Eur J Nucl Med Mol Imaging* **38 Suppl 1**: S10-18.

103. Barat, B, Kenanova, VE, Olafsen, T, and Wu, AM (2011). Evaluation of two internalizing carcinoembryonic antigen reporter genes for molecular imaging. *Mol Imaging Biol* **13**: 526-535.
104. Kenanova, V, Barat, B, Olafsen, T, Chatziioannou, A, Herschman, HR, Braun, J, *et al.* (2009). Recombinant carcinoembryonic antigen as a reporter gene for molecular imaging. *Eur J Nucl Med Mol Imaging* **36**: 104-114.
105. Di Stasi, A, Tey, SK, Dotti, G, Fujita, Y, Kennedy-Nasser, A, Martinez, C, *et al.* (2011). Inducible apoptosis as a safety switch for adoptive cell therapy. *N Engl J Med* **365**: 1673-1683.
106. Itakura, G, Kawabata, S, Ando, M, Nishiyama, Y, Sugai, K, Ozaki, M, *et al.* (2017). Fail-Safe System against Potential Tumorigenicity after Transplantation of iPSC Derivatives. *Stem Cell Reports* **8**: 673-684.
107. Philip, B, Kokalaki, E, Mekkaoui, L, Thomas, S, Straathof, K, Flutter, B, *et al.* (2014). A highly compact epitope-based marker/suicide gene for easier and safer T-cell therapy. *Blood* **124**: 1277-1287.
108. Wang, X, Chang, WC, Wong, CW, Colcher, D, Sherman, M, Ostberg, JR, *et al.* (2011). A transgene-encoded cell surface polypeptide for selection, in vivo tracking, and ablation of engineered cells. *Blood* **118**: 1255-1263.
109. Stavrou, M, Philip, B, Traynor-White, C, Davis, CG, Onuoha, S, Cordoba, S, *et al.* (2018). A Rapamycin-Activated Caspase 9-Based Suicide Gene. *Mol Ther* **26**: 1266-1276.
110. Boardman, DA, Philippeos, C, Fruhwirth, GO, Ibrahim, MA, Hannen, RF, Cooper, D, *et al.* (2017). Expression of a Chimeric Antigen Receptor Specific for Donor HLA Class I Enhances the Potency of Human Regulatory T Cells in Preventing Human Skin Transplant Rejection. *Am J Transplant* **17**: 931-943.
111. Safinia, N, Vaikunthanathan, T, Fraser, H, Thirkell, S, Lowe, K, Blackmore, L, *et al.* (2016). Successful expansion of functional and stable regulatory T cells for immunotherapy in liver transplantation. *Oncotarget* **7**: 7563-7577.
112. Scotta, C, Esposito, M, Fazekasova, H, Fanelli, G, Edozie, FC, Ali, N, *et al.* (2013). Differential effects of rapamycin and retinoic acid on expansion, stability and suppressive qualities of human CD4(+)CD25(+)FOXP3(+) T regulatory cell subpopulations. *Haematologica* **98**: 1291-1299.
113. Caplan, AI (2019). Medicinal signalling cells: they work, so use them. *Nature* **566**: 39.
114. Zhu, J, Zhou, L, and XingWu, F (2006). Tracking neural stem cells in patients with brain trauma. *N Engl J Med* **355**: 2376-2378.
115. Karussis, D, Karageorgiou, C, Vaknin-Dembinsky, A, Gowda-Kurkalli, B, Gomori, JM, Kassis, I, *et al.* (2010). Safety and immunological effects of mesenchymal stem cell transplantation in patients with multiple sclerosis and amyotrophic lateral sclerosis. *Arch Neurol* **67**: 1187-1194.
116. Gholamrezanezhad, A, Mirpour, S, Bagheri, M, Mohamadnejad, M, Alimoghaddam, K, Abdolahzadeh, L, *et al.* (2011). In vivo tracking of 111In-oxine labeled mesenchymal stem cells following infusion in patients with advanced cirrhosis. *Nucl Med Biol* **38**: 961-967.
117. Kang, WJ, Kang, HJ, Kim, HS, Chung, JK, Lee, MC, and Lee, DS (2006). Tissue distribution of 18F-FDG-labeled peripheral hematopoietic stem cells after intracoronary administration in patients with myocardial infarction. *J Nucl Med* **47**: 1295-1301.
118. Hofmann, M, Wollert, KC, Meyer, GP, Menke, A, Arseniev, L, Hertenstein, B, *et al.* (2005). Monitoring of bone marrow cell homing into the infarcted human myocardium. *Circulation* **111**: 2198-2202.

119. Vrtovec, B, Poglajen, G, Lezaic, L, Sever, M, Socan, A, Domanovic, D, *et al.* (2013). Comparison of transendocardial and intracoronary CD34+ cell transplantation in patients with nonischemic dilated cardiomyopathy. *Circulation* **128**: S42-49.
120. Wu, JC, Chen, IY, Sundaresan, G, Min, JJ, De, A, Qiao, JH, *et al.* (2003). Molecular imaging of cardiac cell transplantation in living animals using optical bioluminescence and positron emission tomography. *Circulation* **108**: 1302-1305.
121. Pei, Z, Lan, X, Cheng, Z, Qin, C, Wang, P, He, Y, *et al.* (2012). A multimodality reporter gene for monitoring transplanted stem cells. *Nuclear Medicine and Biology* **39**: 813-820.
122. Lee, AS, Tang, C, Cao, F, Xie, X, van der Bogt, K, Hwang, A, *et al.* (2009). Effects of cell number on teratoma formation by human embryonic stem cells. *Cell Cycle* **8**: 2608-2612.
123. Pomper, MG, Hammond, H, Yu, X, Ye, Z, Foss, CA, Lin, DD, *et al.* (2009). Serial imaging of human embryonic stem-cell engraftment and teratoma formation in live mouse models. *Cell Research* **19**: 370-379.
124. Volarevic, V, Markovic, BS, Gazdic, M, Volarevic, A, Jovicic, N, Arsenijevic, N, *et al.* (2018). Ethical and Safety Issues of Stem Cell-Based Therapy. *Int J Med Sci* **15**: 36-45.
125. Willmann, JK, Paulmurugan, R, Rodriguez-Porcel, M, Stein, W, Brinton, TJ, Connolly, AJ, *et al.* (2009). Imaging Gene Expression in Human Mesenchymal Stem Cells: From Small to Large Animals. *Radiology* **252**: 117-127.
126. Templin, C, Zweigerdt, R, Schwanke, K, Olmer, R, Ghadri, J-R, Emmert, MY, *et al.* (2012). Transplantation and Tracking of Human-Induced Pluripotent Stem Cells in a Pig Model of Myocardial Infarction. *Circulation* **126**: 430-439.
127. Oceguera-Yanez, F, Kim, SI, Matsumoto, T, Tan, GW, Xiang, L, Hatani, T, *et al.* (2016). Engineering the AAVS1 locus for consistent and scalable transgene expression in human iPSCs and their differentiated derivatives. *Methods* **101**: 43-55.
128. Wang, Y, Zhang, WY, Hu, S, Lan, F, Lee, AS, Huber, B, *et al.* (2012). Genome editing of human embryonic stem cells and induced pluripotent stem cells with zinc finger nucleases for cellular imaging. *Circ Res* **111**: 1494-1503.
129. Wolfs, E, Holvoet, B, Ordovas, L, Breuls, N, Helsen, N, Schonberger, M, *et al.* (2017). Molecular Imaging of Human Embryonic Stem Cells Stably Expressing Human PET Reporter Genes After Zinc Finger Nuclease-Mediated Genome Editing. *J Nucl Med* **58**: 1659-1665.
130. Thomson, JA, Itskovitz-Eldor, J, Shapiro, SS, Waknitz, MA, Swiergiel, JJ, Marshall, VS, *et al.* (1998). Embryonic stem cell lines derived from human blastocysts. *Science* **282**: 1145-1147.
131. Tosca, L, Feraud, O, Magniez, A, Bas, C, Griscelli, F, Bennaceur-Griscelli, A, *et al.* (2015). Genomic instability of human embryonic stem cell lines using different passaging culture methods. *Molecular Cytogenetics* **8**: 30.
132. Huang, CY, Liu, CL, Ting, CY, Chiu, YT, Cheng, YC, Nicholson, MW, *et al.* (2019). Human iPSC banking: barriers and opportunities. *J Biomed Sci* **26**: 87.
133. Charoenphun, P, Meszaros, LK, Chuamsaamarkkee, K, Sharif-Paghaleh, E, Ballinger, JR, Ferris, TJ, *et al.* (2015). [(89)Zr]oxinate4 for long-term in vivo cell tracking by positron emission tomography. *Eur J Nucl Med Mol Imaging* **42**: 278-287.
134. Sato, N, Wu, H, Asiedu, KO, Szajek, LP, Griffiths, GL, and Choyke, PL (2015). (89)Zr-Oxine Complex PET Cell Imaging in Monitoring Cell-based Therapies. *Radiology* **275**: 490-500.
135. Man, F, Lim, L, Volpe, A, Gabizon, A, Shmeeda, H, Draper, B, *et al.* (2019). In Vivo PET Tracking of (89)Zr-Labeled Vgamma9Vdelta2 T Cells to Mouse Xenograft Breast Tumors Activated with Liposomal Alendronate. *Mol Ther* **27**: 219-229.

136. Cherry, SR, Jones, T, Karp, JS, Qi, J, Moses, WW, and Badawi, RD (2018). Total-Body PET: Maximizing Sensitivity to Create New Opportunities for Clinical Research and Patient Care. *J Nucl Med* **59**: 3-12.
137. Eyquem, J, Mansilla-Soto, J, Giavridis, T, van der Stegen, SJ, Hamieh, M, Cunanan, KM, *et al.* (2017). Targeting a CAR to the TRAC locus with CRISPR/Cas9 enhances tumour rejection. *Nature* **543**: 113-117.
138. Kotterman, MA, Chalberg, TW, and Schaffer, DV (2015). Viral Vectors for Gene Therapy: Translational and Clinical Outlook. *Annu Rev Biomed Eng* **17**: 63-89.
139. Martinez, M, and Moon, EK (2019). CAR T Cells for Solid Tumors: New Strategies for Finding, Infiltrating, and Surviving in the Tumor Microenvironment. *Front Immunol* **10**: 128.
140. Andreyev, A, and Celler, A (2011). Dual-isotope PET using positron-gamma emitters. *Phys Med Biol* **56**: 4539-4556.
141. Cal-Gonzalez, J, Lage, E, Herranz, E, Vicente, E, Udias, JM, Moore, SC, *et al.* (2015). Simulation of triple coincidences in PET. *Phys Med Biol* **60**: 117-136.
142. Lage, E, Parot, V, Moore, SC, Sitek, A, Udias, JM, Dave, SR, *et al.* (2015). Recovery and normalization of triple coincidences in PET. *Med Phys* **42**: 1398-1410.
143. Naumova, AV, Modo, M, Moore, A, Murry, CE, and Frank, JA (2014). Clinical imaging in regenerative medicine. *Nat Biotechnol* **32**: 804-818.
144. Afzali, B, Edozie, FC, Fazekasova, H, Scotta, C, Mitchell, PJ, Canavan, JB, *et al.* (2013). Comparison of regulatory T cells in hemodialysis patients and healthy controls: implications for cell therapy in transplantation. *Clin J Am Soc Nephrol* **8**: 1396-1405.
145. Alhadj Ali, M, Liu, YF, Arif, S, Tatovic, D, Shariff, H, Gibson, VB, *et al.* (2017). Metabolic and immune effects of immunotherapy with proinsulin peptide in human new-onset type 1 diabetes. *Sci Transl Med* **9**.
146. Smith, EL, and Peakman, M (2018). Peptide Immunotherapy for Type 1 Diabetes-Clinical Advances. *Front Immunol* **9**: 392.
147. Chataway, J, Martin, K, Barrell, K, Sharrack, B, Stolt, P, Wraith, DC, *et al.* (2018). Effects of ATX-MS-1467 immunotherapy over 16 weeks in relapsing multiple sclerosis. *Neurology* **90**: e955-e962.
148. Hotchkiss, RS, and Moldawer, LL (2014). Parallels between cancer and infectious disease. *N Engl J Med* **371**: 380-383.
149. Farhadi, A, Ho, GH, Sawyer, DP, Bourdeau, RW, and Shapiro, MG (2019). Ultrasound imaging of gene expression in mammalian cells. *Science* **365**: 1469-1475.
150. Zabow, G, Dodd, S, Moreland, J, and Koretsky, A (2008). Micro-engineered local field control for high-sensitivity multispectral MRI. *Nature* **453**: 1058.
151. Tjuvajev, JG, Doubrovin, M, Akhurst, T, Cai, S, Balatoni, J, Alauddin, MM, *et al.* (2002). Comparison of radiolabeled nucleoside probes (FIAU, FHBG, and FHPG) for PET imaging of HSV1-tk gene expression. *J Nucl Med* **43**: 1072-1083.
152. Dai, G, Levy, O, and Carrasco, N (1996). Cloning and characterization of the thyroid iodide transporter. *Nature* **379**: 458-460.
153. Khoshnevisan, A, Jauregui-Osoro, M, Shaw, K, Torres, JB, Young, JD, Ramakrishnan, NK, *et al.* (2016). [(18)F]tetrafluoroborate as a PET tracer for the sodium/iodide symporter: the importance of specific activity. *EJNMMI Res* **6**: 34.
154. Moroz, MA, Serganova, I, Zanzonico, P, Ageyeva, L, Beresten, T, Dyomina, E, *et al.* (2007). Imaging hNET reporter gene expression with 124I-MIBG. *J Nucl Med* **48**: 827-836.
155. Martin Pulé (London), ABL, Louise Kiru (London), Mark Lythgoe (London), Adrien Peters (Brighton) (2015). Detecting a Therapeutic Cell. *Publication number: 20170056534*.

156. Haywood, T, Beinat, C, Gowrishankar, G, Patel, CB, Alam, IS, Murty, S, *et al.* (2019). Positron emission tomography reporter gene strategy for use in the central nervous system. *Proc Natl Acad Sci U S A* **116**: 11402-11407.
157. Ponomarev, V, Doubrovin, M, Shavrin, A, Serganova, I, Beresten, T, Ageyeva, L, *et al.* (2007). A human-derived reporter gene for noninvasive imaging in humans: mitochondrial thymidine kinase type 2. *J Nucl Med* **48**: 819-826.
158. Likar, Y, Zurita, J, Dobrenkov, K, Shenker, L, Cai, S, Neschadim, A, *et al.* (2010). A new pyrimidine-specific reporter gene: a mutated human deoxycytidine kinase suitable for PET during treatment with acycloguanosine-based cytotoxic drugs. *J Nucl Med* **51**: 1395-1403.
159. Rogers, BE, McLean, SF, Kirkman, RL, Della Manna, D, Bright, SJ, Olsen, CC, *et al.* (1999). In vivo localization of [(111)In]-DTPA-D-Phe1-octreotide to human ovarian tumor xenografts induced to express the somatostatin receptor subtype 2 using an adenoviral vector. *Clin Cancer Res* **5**: 383-393.
160. Chaudhuri, TR, Rogers, BE, Buchsbaum, DJ, Mountz, JM, and Zinn, KR (2001). A noninvasive reporter system to image adenoviral-mediated gene transfer to ovarian cancer xenografts. *Gynecol Oncol* **83**: 432-438.
161. Zinn KR, BD, Chaudhuri TR, Mountz JM, Grizzle WE,, and BE., R (2000). Simultaneous in vivo imaging of thymidine kinase and somatostatin receptor expression after gene transfer with an adenoviral vector encoding both genes. *Mol Ther* **1:S44**.
162. Rogers, BE, Zinn, KR, and Buchsbaum, DJ (2000). Gene transfer strategies for improving radiolabeled peptide imaging and therapy. *Q J Nucl Med* **44**: 208-223.
163. MacLaren, DC, Gambhir, SS, Satyamurthy, N, Barrio, JR, Sharfstein, S, Toyokuni, T, *et al.* (1999). Repetitive, non-invasive imaging of the dopamine D2 receptor as a reporter gene in living animals. *Gene Ther* **6**: 785-791.
164. Liang, Q, Satyamurthy, N, Barrio, JR, Toyokuni, T, Phelps, MP, Gambhir, SS, *et al.* (2001). Noninvasive, quantitative imaging in living animals of a mutant dopamine D2 receptor reporter gene in which ligand binding is uncoupled from signal transduction. *Gene Ther* **8**: 1490-1498.
165. Satyamurthy, N, Barrio, JR, Bida, GT, Huang, SC, Mazziotta, JC, and Phelps, ME (1990). 3-(2'-[18F]fluoroethyl)spiperone, a potent dopamine antagonist: synthesis, structural analysis and in-vivo utilization in humans. *Int J Rad Appl Instrum A* **41**: 113-129.
166. Hwang, DW, Kang, JH, Chang, YS, Jeong, JM, Chung, JK, Lee, MC, *et al.* (2007). Development of a dual membrane protein reporter system using sodium iodide symporter and mutant dopamine D2 receptor transgenes. *J Nucl Med* **48**: 588-595.
167. Weissleder, R, Moore, A, Mahmood, U, Bhorade, R, Benveniste, H, Chiocca, EA, *et al.* (2000). In vivo magnetic resonance imaging of transgene expression. *Nat Med* **6**: 351-355.
168. Hammarstrom, S (1999). The carcinoembryonic antigen (CEA) family: structures, suggested functions and expression in normal and malignant tissues. *Semin Cancer Biol* **9**: 67-81.
169. Hong, H, Sun, J, and Cai, W (2008). Radionuclide-Based Cancer Imaging Targeting the Carcinoembryonic Antigen. *Biomark Insights* **3**: 435-451.
170. Girgis, MD, Olafsen, T, Kenanova, V, McCabe, KE, Wu, AM, and Tomlinson, JS (2011). Targeting CEA in Pancreas Cancer Xenografts with a Mutated scFv-Fc Antibody Fragment. *EJNMMI Res* **1**: 24.
171. Cohen, B, Dafni, H, Meir, G, Harmelin, A, and Neeman, M (2005). Ferritin as an endogenous MRI reporter for noninvasive imaging of gene expression in C6 glioma tumors. *Neoplasia* **7**: 109-117.
172. Genove, G, DeMarco, U, Xu, H, Goins, WF, and Ahrens, ET (2005). A new transgene reporter for in vivo magnetic resonance imaging. *Nat Med* **11**: 450-454.

173. Louie, AY, Hüber, MM, Ahrens, ET, Rothbächer, U, Moats, R, Jacobs, RE, *et al.* (2000). In vivo visualization of gene expression using magnetic resonance imaging. *Nature biotechnology* **18**: 321.
174. Liu, L, and Mason, RP (2010). Imaging β-galactosidase activity in human tumor xenografts and transgenic mice using a chemiluminescent substrate. *PLoS One* **5**: e12024.
175. Li, L, Zemp, RJ, Lungu, GF, Stoica, G, and Wang, LV (2007). Photoacoustic imaging of lacZ gene expression in vivo. *Journal of biomedical optics* **12**: 020504.
176. Guo, Y, Hui, C-Y, Liu, L, Zheng, H-Q, and Wu, H-M (2019). Improved Monitoring of Low-Level Transcription in Escherichia coli by a β-Galactosidase α-Complementation System. *Frontiers in Microbiology* **10**.
177. Krueger, MA, Cotton, JM, Zhou, B, Wolter, K, Schwenck, J, Kuehn, A, *et al.* (2019). Abstract 1146: [18F]FPyGal: A novel ß-galactosidase specific PET tracer for in vivo imaging of tumor senescence. *Cancer Research* **79**: 1146-1146.
178. Fowler, AV, and Zabin, I (1977). The amino acid sequence of beta-galactosidase of Escherichia coli. *Proceedings of the National Academy of Sciences of the United States of America* **74**: 1507-1510.
179. Green, O, Gnaim, S, Blau, R, Eldar-Boock, A, Satchi-Fainaro, R, and Shabat, D (2017). Near-Infrared Dioxetane Luminophores with Direct Chemiluminescence Emission Mode. *Journal of the American Chemical Society* **139**: 13243-13248.
180. Sellmyer, MA, Richman, SA, Lohith, K, Hou, C, Weng, C-C, Mach, RH, *et al.* (2019). Imaging CAR T Cell Trafficking with eDHFR as a PET Reporter Gene. *Molecular Therapy*.
181. Sellmyer, MA, Lee, I, Hou, C, Lieberman, BP, Zeng, C, Mankoff, DA, *et al.* (2017). Quantitative PET Reporter Gene Imaging with [11C] Trimethoprim. *Molecular Therapy* **25**: 120-126.
182. Tjuvajev, JG, Stockhammer, G, Desai, R, Uehara, H, Watanabe, K, Gansbacher, B, *et al.* (1995). Imaging the expression of transfected genes in vivo. *Cancer research* **55**: 6126-6132.
183. Jang, SJ, Kang, JH, Kim, KI, Lee, TS, Lee, YJ, Lee, KC, *et al.* (2010). Application of bioluminescence imaging to therapeutic intervention of herpes simplex virus type I–Thymidine kinase/ganciclovir in glioma. *Cancer letters* **297**: 84-90.
184. Jang, SJ, Lee, YJ, Lim, S, Kim, KI, Lee, KC, An, GI, *et al.* (2012). Imaging of a localized bacterial infection with endogenous thymidine kinase using radioisotope-labeled nucleosides. *International Journal of Medical Microbiology* **302**: 101-107.
185. Park, JH, Kim, KI, Lee, KC, Lee, YJ, Lee, TS, Chung, WS, *et al.* (2015). Assessment of α-fetoprotein targeted HSV1-tk expression in hepatocellular carcinoma with in vivo imaging. *Cancer Biotherapy and Radiopharmaceuticals* **30**: 8-15.
186. Seo, M-J, Park, JH, Lee, KC, Lee, YJ, Lee, TS, Choi, TH, *et al.* (2019). Small Animal PET Imaging of hTERT RNA-Targeted HSV1-tk Gene Expression with Trans-Splicing Ribozyme. *Cancer biotherapy & radiopharmaceuticals*.
187. Uchibori, R, Teruya, T, Ido, H, Ohmine, K, Sehara, Y, Urabe, M, *et al.* (2019). Functional Analysis of an Inducible Promoter Driven by Activation Signals from a Chimeric Antigen Receptor. *Molecular Therapy-Oncolytics* **12**: 16-25.
188. Nakajima, Y, Yamazaki, T, Nishii, S, Noguchi, T, Hoshino, H, Niwa, K, *et al.* (2010). Enhanced Beetle Luciferase for High-Resolution Bioluminescence Imaging. *PLOS ONE* **5**: e10011.
189. Nishiguchi, T, Yamada, T, Nasu, Y, Ito, M, Yoshimura, H, and Ozawa, T (2015). Development of red-shifted mutants derived from luciferase of Brazilian click beetle *Pyrearinus termitilluminans*. *Journal of Biomedical Optics* **20**: 1-7, 7.

190. Morikawa, K, Nakamura, K, Suyama, Y, Yamamoto, K, Fukuoka, K, Yagi, S, *et al.* (2019). Novel dual-reporter transgenic rodents enable cell tracking in animal models of stem cell transplantation. *Biochemistry and Biophysics Reports* **18**: 100645.
191. Mezzanotte, L, van't Root, M, Karatas, H, Goun, EA, and Löwik, CW (2017). In vivo molecular bioluminescence imaging: new tools and applications. *Trends in biotechnology* **35**: 640-652.
192. Weihs, F, and Dacres, H (2019). Red-shifted bioluminescence Resonance Energy Transfer: Improved tools and materials for analytical in vivo approaches. *TRAC-TRENDS IN ANALYTICAL CHEMISTRY* **116**: 61-73.
193. Aswendt, M, Vogel, S, Schäfer, C, Jathoul, A, Pule, M, and Hoehn, M (2019). Quantitative i*n vivo* dual-color bioluminescence imaging in the mouse brain. *Neurophotonics* **6**: 1-11, 11.
194. Inoue, Y, Sheng, F, Kiryu, S, Watanabe, M, Ratanakanit, H, Izawa, K, *et al.* (2011). Gaussia luciferase for bioluminescence tumor monitoring in comparison with firefly luciferase. *Molecular imaging* **10**: 7290.2010. 00057.
195. Tannous, BA (2009). Gaussia luciferase reporter assay for monitoring biological processes in culture and in vivo. *Nature protocols* **4**: 582.
196. Hunt, EA, Moutsiopoulou, A, Ioannou, S, Ahern, K, Woodward, K, Dikici, E, *et al.* (2016). Truncated Variants of Gaussia Luciferase with Tyrosine Linker for Site-Specific Bioconjugate Applications. *Scientific Reports* **6**: 26814.
197. Zhang, Y, Wang, C, Gao, N, Zhang, X, Yu, X, Xu, J, *et al.* (2019). Determination of neutralization activities by a new versatile assay using an HIV-1 genome carrying the Gaussia luciferase gene. *Journal of Virological Methods* **267**: 22-28.
198. Mezzanotte, L, An, N, Mol, IM, Löwik, CW, and Kaijzel, EL (2014). A new multicolor bioluminescence imaging platform to investigate NF-κB activity and apoptosis in human breast cancer cells. *PloS one* **9**: e85550.
199. Hall, MP, Unch, J, Binkowski, BF, Valley, MP, Butler, BL, Wood, MG, *et al.* (2012). Engineered Luciferase Reporter from a Deep Sea Shrimp Utilizing a Novel Imidazopyrazinone Substrate. *ACS Chemical Biology* **7**: 1848-1857.
200. La Barbera, G, Capriotti, AL, Michelini, E, Piovesana, S, Calabretta, MM, Zenezini Chiozzi, R, *et al.* (2017). Proteomic analysis and bioluminescent reporter gene assays to investigate effects of simulated microgravity on Caco-2 cells. *PROTEOMICS* **17**: 1700081.
201. Schaub, FX, Reza, MS, Flaveny, CA, Li, W, Musicant, AM, Hoxha, S, *et al.* (2015). Fluorophore-NanoLuc BRET Reporters Enable Sensitive In Vivo Optical Imaging and Flow Cytometry for Monitoring Tumorigenesis. *Cancer Research* **75**: 5023-5033.
202. Germain-Genevois, C, Garandeau, O, and Couillaud, F (2016). Detection of Brain Tumors and Systemic Metastases Using NanoLuc and Fluc for Dual Reporter Imaging. *Molecular Imaging and Biology* **18**: 62-69.
203. Lorenz, WW, McCann, RO, Longiaru, M, and Cormier, MJ (1991). Isolation and expression of a cDNA encoding Renilla reniformis luciferase. *Proceedings of the National Academy of Sciences* **88**: 4438-4442.
204. Loening, AM, Fenn, TD, Wu, AM, and Gambhir, SS (2006). Consensus guided mutagenesis of Renilla luciferase yields enhanced stability and light output. *Protein Engineering, Design and Selection* **19**: 391-400.
205. Zurkiya, O, Chan, AWS, and Hu, X (2008). MagA is sufficient for producing magnetic nanoparticles in mammalian cells, making it an MRI reporter. *Magnetic Resonance in Medicine* **59**: 1225-1231.

206. Cho, IK, Moran, SP, Paudyal, R, Piotrowska-Nitsche, K, Cheng, P-H, Zhang, X, *et al.* (2014). Longitudinal monitoring of stem cell grafts in vivo using magnetic resonance imaging with inducible maga as a genetic reporter. *Theranostics* **4**: 972-989.
207. Nakamura, C, Burgess, JG, Sode, K, and Matsunaga, T (1995). An iron-regulated gene, magA, encoding an iron transport protein of Magnetospirillum sp. strain AMB-1. *Journal of Biological Chemistry* **270**: 28392-28396.
208. Wu, M-R, Huang, Y-Y, and Hsiao, J-K (2019). Use of Indocyanine Green (ICG), a Medical Near Infrared Dye, for Enhanced Fluorescent Imaging—Comparison of Organic Anion Transporting Polypeptide 1B3 (OATP1B3) and Sodium-Taurocholate Cotransporting Polypeptide (NTCP) Reporter Genes. *Molecules* **24**: 2295.
209. Gilad, AA, McMahon, MT, Walczak, P, Winnard Jr, PT, Raman, V, Van Laarhoven, HW, *et al.* (2007). Artificial reporter gene providing MRI contrast based on proton exchange. *Nature biotechnology* **25**: 217.
210. Farrar, CT, Buhrman, JS, Liu, G, Kleijn, A, Lamfers, ML, McMahon, MT, *et al.* (2015). Establishing the lysine-rich protein CEST reporter gene as a CEST MR imaging detector for oncolytic virotherapy. *Radiology* **275**: 746-754.
211. Kremers, G-J, Hazelwood, KL, Murphy, CS, Davidson, MW, and Piston, DW (2009). Photoconversion in orange and red fluorescent proteins. *Nature methods* **6**: 355.
212. Lin, MZ, McKeown, MR, Ng, H-L, Aguilera, TA, Shaner, NC, Campbell, RE, *et al.* (2009). Autofluorescent proteins with excitation in the optical window for intravital imaging in mammals. *Chemistry & biology* **16**: 1169-1179.
213. Merzlyak, EM, Goedhart, J, Shcherbo, D, Bulina, ME, Shcheglov, AS, Fradkov, AF, *et al.* (2007). Bright monomeric red fluorescent protein with an extended fluorescence lifetime. *Nature methods* **4**: 555.
214. Liu, M, Schmitner, N, Sandrian, MG, Zabihian, B, Hermann, B, Salvenmoser, W, *et al.* (2013). In vivo three dimensional dual wavelength photoacoustic tomography imaging of the far red fluorescent protein E2-Crimson expressed in adult zebrafish. *Biomedical optics express* **4**: 1846-1855.
215. Zhou, J, Sharkey, J, Shukla, R, Plagge, A, and Murray, P (2018). Assessing the effectiveness of a far-red fluorescent reporter for tracking stem cells in vivo. *International journal of molecular sciences* **19**: 19.
216. Shcherbakova, DM, and Verkhusha, VV (2013). Near-infrared fluorescent proteins for multicolor in vivo imaging. *Nature methods* **10**: 751.
217. Shu, X, Royant, A, Lin, MZ, Aguilera, TA, Lev-Ram, V, Steinbach, PA, *et al.* (2009). Mammalian expression of infrared fluorescent proteins engineered from a bacterial phytochrome. *Science* **324**: 804-807.
218. Filonov, GS, Piatkevich, KD, Ting, L-M, Zhang, J, Kim, K, and Verkhusha, VV (2011). Bright and stable near-infrared fluorescent protein for in vivo imaging. *Nature biotechnology* **29**: 757.
219. Deliolanis, NC, Ale, A, Morscher, S, Burton, NC, Schaefer, K, Radrich, K, *et al.* (2014). Deep-tissue reporter-gene imaging with fluorescence and optoacoustic tomography: a performance overview. *Molecular imaging and biology* **16**: 652-660.
220. Wang, H, Willershäuser, M, Karlas, A, Gorpas, D, Reber, J, Ntziachristos, V, *et al.* (2019). A dual Ucp1 reporter mouse model for imaging and quantitation of brown and brite fat recruitment. *Molecular Metabolism* **20**: 14-27.
221. Isomura, M, Yamada, K, Noguchi, K, and Nishizono, A (2017). Near-infrared fluorescent protein iRFP720 is optimal for in vivo fluorescence imaging of rabies virus infection. *Journal of General Virology* **98**: 2689-2698.

222. Fukuda, A, Honda, S, Fujioka, N, Sekiguchi, Y, Mizuno, S, Miwa, Y, *et al.* (2019). Non-invasive in vivo imaging of UCP1 expression in live mice via near-infrared fluorescent protein iRFP720. *PLOS ONE* **14**: e0225213.
223. Bourdeau, RW, Lee-Gosselin, A, Lakshmanan, A, Farhadi, A, Kumar, SR, Nety, SP, *et al.* (2018). Acoustic reporter genes for noninvasive imaging of microorganisms in mammalian hosts. *Nature* **553**: 86.
224. Farhadi, A, Ho, GH, Sawyer, DP, Bourdeau, RW, and Shapiro, MG (2019). Ultrasound imaging of gene expression in mammalian cells. *Science* **365**: 1469.
225. McCracken, MN, Gschweng, EH, Nair-Gill, E, McLaughlin, J, Cooper, AR, Riedinger, M, *et al.* (2013). Long-term in vivo monitoring of mouse and human hematopoietic stem cell engraftment with a human positron emission tomography reporter gene. *Proceedings of the National Academy of Sciences* **110**: 1857-1862.
226. Kim, YH, Lee, DS, Kang, JH, Lee, YJ, Chung, J-K, Roh, J-K, *et al.* (2005). Reversing the silencing of reporter sodium/iodide symporter transgene for stem cell tracking. *Journal of Nuclear Medicine* **46**: 305-311.
227. Schug, C, Urnauer, S, Jaeckel, C, Schmohl, KA, Tutter, M, Steiger, K, *et al.* (2019). TGFB1-driven mesenchymal stem cell-mediated NIS gene transfer. *Endocr Relat Cancer* **26**: 89-101.
228. Dwyer, RM, Ryan, J, Havelin, RJ, Morris, JC, Miller, BW, Liu, Z, *et al.* (2011). Mesenchymal Stem Cell-mediated delivery of the sodium iodide symporter supports radionuclide imaging and treatment of breast cancer. *Stem Cells* **29**: 1149-1157.
229. Love, Z, Wang, F, Dennis, J, Awadallah, A, Salem, N, Lin, Y, *et al.* (2007). Imaging of mesenchymal stem cell transplant by bioluminescence and PET. *Journal of Nuclear Medicine* **48**: 2011-2020.
230. Schönitzer, V, Haasters, F, Käsbauer, S, Ulrich, V, Mille, E, Gildehaus, FJ, *et al.* (2014). In vivo mesenchymal stem cell tracking with PET using the dopamine type 2 receptor and 18F-fallypride. *Journal of Nuclear Medicine* **55**: 1342-1347.
231. Swijnenburg, R-J, Schrepfer, S, Govaert, JA, Cao, F, Ransohoff, K, Sheikh, AY, *et al.* (2008). Immunosuppressive therapy mitigates immunological rejection of human embryonic stem cell xenografts. *Proceedings of the National Academy of Sciences* **105**: 12991-12996.
232. Daadi, MM, Hu, S, Klausner, J, Li, Z, Sofilos, M, Sun, G, *et al.* (2013). Imaging neural stem cell graft-induced structural repair in stroke. *Cell transplantation* **22**: 881-892.
233. Priddle, H, Grabowska, A, Morris, T, Clarke, PA, McKenzie, AJ, Sottile, V, *et al.* (2009). Bioluminescence imaging of human embryonic stem cells transplanted in vivo in murine and chick models. *Cloning and stem cells* **11**: 259-267.
234. Wolfs, E, Holvoet, B, Ordovas, L, Breuls, N, Helsen, N, Schönberger, M, *et al.* (2017). Molecular Imaging of Human Embryonic Stem Cells Stably Expressing Human PET Reporter Genes After Zinc Finger Nuclease–Mediated Genome Editing. *Journal of Nuclear Medicine* **58**: 1659-1665.
235. Wang, Y, Zhang, WY, Hu, S, Lan, F, Lee, AS, Huber, B, *et al.* (2012). Genome editing of human embryonic stem cells and induced pluripotent stem cells with zinc finger nucleases for cellular imaging. *Circulation research* **111**: 1494-1503.
236. Tian, X, Hexum, MK, Penchev, VR, Taylor, RJ, Shultz, LD, and Kaufman, DS (2009). Bioluminescent Imaging Demonstrates That Transplanted Human Embryonic Stem Cell-Derived CD34+ Cells Preferentially Develop into Endothelial Cells. *Stem Cells* **27**: 2675-2685.
237. Laurila, JP, Laatikainen, L, Castellone, MD, Trivedi, P, Heikkila, J, Hinkkanen, A, *et al.* (2009). Human embryonic stem cell-derived mesenchymal stromal cell transplantation in a rat hind limb injury model. Taylor & Francis.

238. Korn, T, Mitsdoerffer, M, Croxford, AL, Awasthi, A, Dardalhon, VA, Galileos, G, *et al.* (2008). IL-6 controls Th17 immunity in vivo by inhibiting the conversion of conventional T cells into Foxp3+ regulatory T cells. *Proc Natl Acad Sci U S A* **105**: 18460-18465.
239. Bradbury, MS, Panagiotakos, G, Chan, BK, Tomishima, M, Zanzonico, P, Vider, J, *et al.* (2007). Optical bioluminescence imaging of human ES cell progeny in the rodent CNS. *Journal of neurochemistry* **102**: 2029-2039.
240. Barberi, T, Bradbury, M, Dincer, Z, Panagiotakos, G, Socci, ND, and Studer, L (2007). Derivation of engraftable skeletal myoblasts from human embryonic stem cells. *Nature medicine* **13**: 642.
241. Pomper, MG, Hammond, H, Yu, X, Ye, Z, Foss, CA, Lin, DD, *et al.* (2009). Serial imaging of human embryonic stem-cell engraftment and teratoma formation in live mouse models. *Cell research* **19**: 370.
242. Lopez-Yrigoyen, M, Fidanza, A, Cassetta, L, Axton, RA, Taylor, AH, Meseguer-Ripolles, J, *et al.* (2018). A human iPSC line capable of differentiating into functional macrophages expressing ZsGreen: a tool for the study and in vivo tracking of therapeutic cells. *Philosophical Transactions of the Royal Society B: Biological Sciences* **373**: 20170219.
243. Ashmore-Harris, C, Blackford, SJ, Grimsdell, B, Kurtys, E, Glatz, MC, Rashid, TS, *et al.* (2019). Reporter gene-engineering of human induced pluripotent stem cells during differentiation renders in vivo traceable hepatocyte-like cells accessible. *Stem cell research* **41**: 101599.
244. Itakura, G, Kobayashi, Y, Nishimura, S, Iwai, H, Takano, M, Iwanami, A, *et al.* (2015). Controlling immune rejection is a fail-safe system against potential tumorigenicity after human iPSC-derived neural stem cell transplantation. *PloS one* **10**: e0116413.
245. Rufaihah, AJ, Huang, NF, Jamé, S, Lee, JC, Nguyen, HN, Byers, B, *et al.* (2011). Endothelial cells derived from human iPSCS increase capillary density and improve perfusion in a mouse model of peripheral arterial disease. *Arteriosclerosis, thrombosis, and vascular biology* **31**: e72-e79.
246. Templin, C, Zweigerdt, R, Schwanke, K, Olmer, R, Ghadri, J-R, Emmert, MY, *et al.* (2012). Transplantation and tracking of human-induced pluripotent stem cells in a pig model of myocardial infarction: assessment of cell survival, engraftment, and distribution by hybrid single photon emission computed tomography/computed tomography of sodium iodide symporter transgene expression. *Circulation* **126**: 430-439.
247. Bedel, A, Beliveau, F, Lamrissi- Garcia, I, Rousseau, B, Moranvillier, I, Rucheton, B, *et al.* (2017). Preventing pluripotent cell teratoma in regenerative medicine applied to hematology disorders. *Stem cells translational medicine* **6**: 382-393.
248. Mattapally, S, Zhu, W, Fast, VG, Gao, L, Worley, C, Kannappan, R, *et al.* (2018). Spheroids of cardiomyocytes derived from human-induced pluripotent stem cells improve recovery from myocardial injury in mice. *American Journal of Physiology-Heart and Circulatory Physiology* **315**: H327-H339.

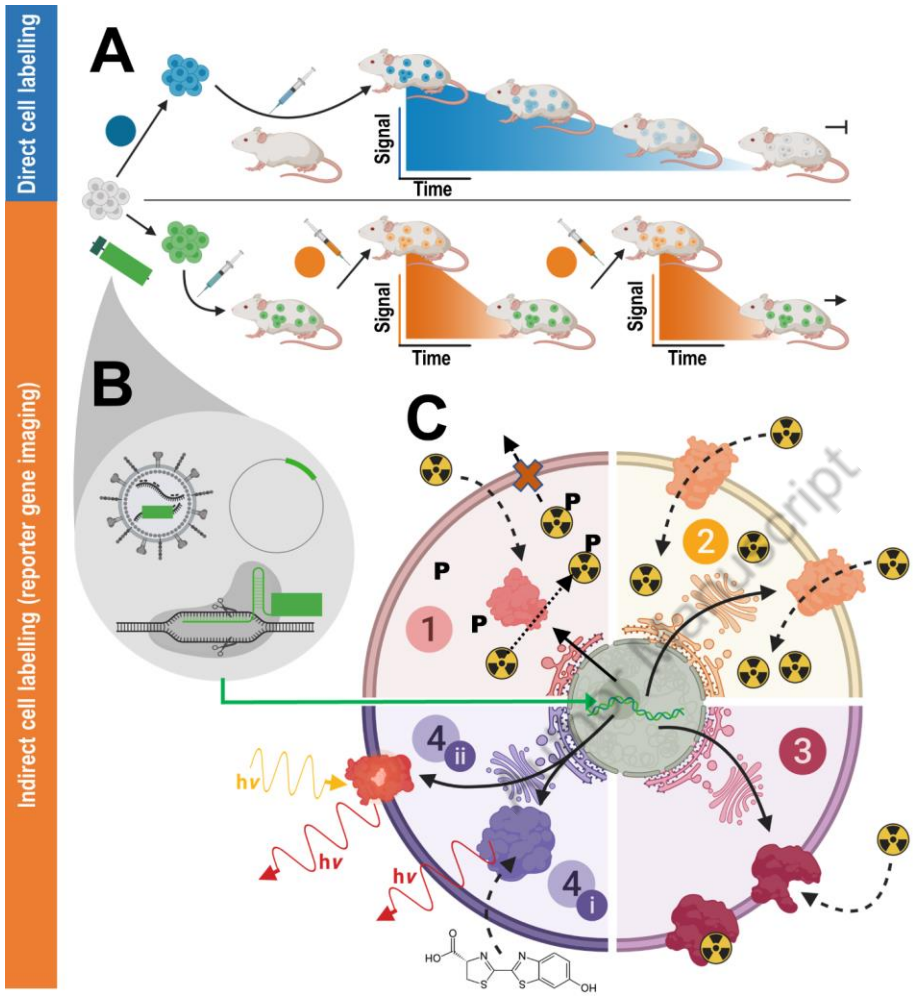

Figure 1. *In vivo* cell tracking using reporter genes. | (A/blue) Direct cell labelling employs *ex vivo* labelled cells that are administered to animals and can be tracked until cells lose their labels (depicted using blue signal *versus* time cartoon plots) *e.g.* through label efflux, *via* label dilution in fast-growing cells, or radioisotope decay if radiotracers are used. **(B/orange) Indirect cell labelling** requires cells that have been genetically manipulated to express a reporter gene (green). The genetic engineering options frequently employed in reporter gene applications include viruses (*e.g.* lentiviruses,

γ--retroviruses), gene editing or episomal plasmids (see cartoons within grey drop). The cells are imaged using the features of the reporter gene, which renders the cells traceable *in vivo*. Cells are detected *in vivo* through molecular probe administration (depicted using orange signal *versus* time cartoon plots); if radiotracers are used, their half-life is short to enable short repeat-imaging intervals and keep administered doses low. Reporter gene imaging does not suffer from label dilution in fast growing cells, hence permits much longer, theoretically indefinite observation times. **(C) Molecular imaging mechanisms of frequently used reporter genes. (C/1)** Enzymes entrapping molecular probes (light red): these reporter enzymes entrap a substrate that is already detectable by imaging. A frequent mechanism for this entrapment relies on phosphorylation of a substrate that has either actively or passively entered the cell, and upon phosphorylation can no longer leave the cell. Examples are nucleoside kinases for such as HSV1-*tk*. **(C/2)** Transporter proteins (yellow): these reporters are expressed at the plasma membrane of cells and each expressed reporter can transport several labelling agent molecules into the cell, which constitutes a signal amplification mechanism. The radionuclide transporters NIS and NET belong to this class of reporters. **(C/3)** Cell surface molecules (pink): these reporters are expressed at the plasma membrane of cells and molecular probes bind directly to them; minor levels of signal amplification are theoretically possible if several labels bind directly to each reporter protein, or if several labels could be fused to a reporter binding molecule; however, signal amplification is inferior compared to transporters and often they are used with a 1:1 stoichiometry. Examples for this reporter class are tPSMA^{N9Del} and SSTR2. **(C/4)** Signal generating proteins (purple). **(C/4i)** Enzyme based reporters bind to their substrate and catalyse the production of a detectable signal. Examples are luciferases, which convert an externally supplied chemical substrate into detectable light (hv). **(C/4ii)** Fluorescent proteins contain an intrinsic fluorescence-generating moiety if appropriately excited by light. Fluorophore excitation results in emission of detectable longer wavelength/red-shifted light. For details and literature references to relevant reporter genes see Tab.1-2. The figure was generated using Biorender.com.

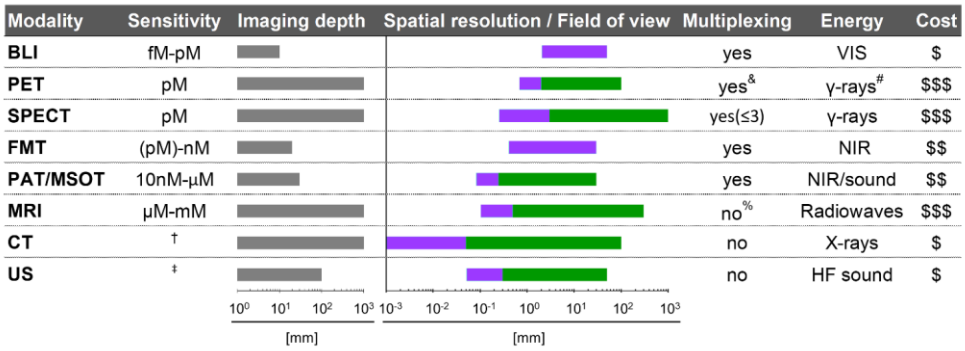

Figure 2. Properties of various whole-body imaging modalities | Imaging modalities are ordered according to their molecular detection sensitivities with achievable imaging depth shown in gray alongside. Achievable spatial resolution (left end) and fields of view (right end) are shown in cyan/green. Where bars are green, they overlay purple bars and indicate the same parameters but achievable with instruments available for clinical imaging. Instrument cost estimations are classified as ($) <130,000 $, ($$) 130-300,000 $ and ($$$) >300,000 $.

† Contrast agents sometimes used to obtain different anatomical/functional information.

‡ Sensitivity is highly dependent on contrast forming features/contrast agent. A new mammalian reporter gene for US imaging was recently reported to detect a minimum of 135 gas vesicles per voxel with dimensions of 100µm [149].

& Dual isotope PET is feasible but not routinely in use; it requires two tracers, one with a positron emitter (*e.g.* ^{18}F, ^{89}Zr) and the other with a positron-gamma emitter (*e.g.* ^{124}I, ^{76}Br, ^{86}Y), and is based on recent reconstruction algorithms to differentiate the two isotopes based on the prompt-gamma emission [140-142].

% Multichannel MRI imaging has been shown to be feasible [150] but is not routinely available.

Generated by positron annihilation (511keV).

Abbreviations: bioluminescence imaging (BLI), positron emission tomography (PET), single photon emission computed tomography (SPECT), fluorescence molecular tomography (FMT), photoacoustic tomography/multispectral optoacoustic tomography (PAT/MSOT), magnetic resonance imaging (MRI), near-infrared (NIR), visible (VIS), high frequency (HF), computed tomography (CT).

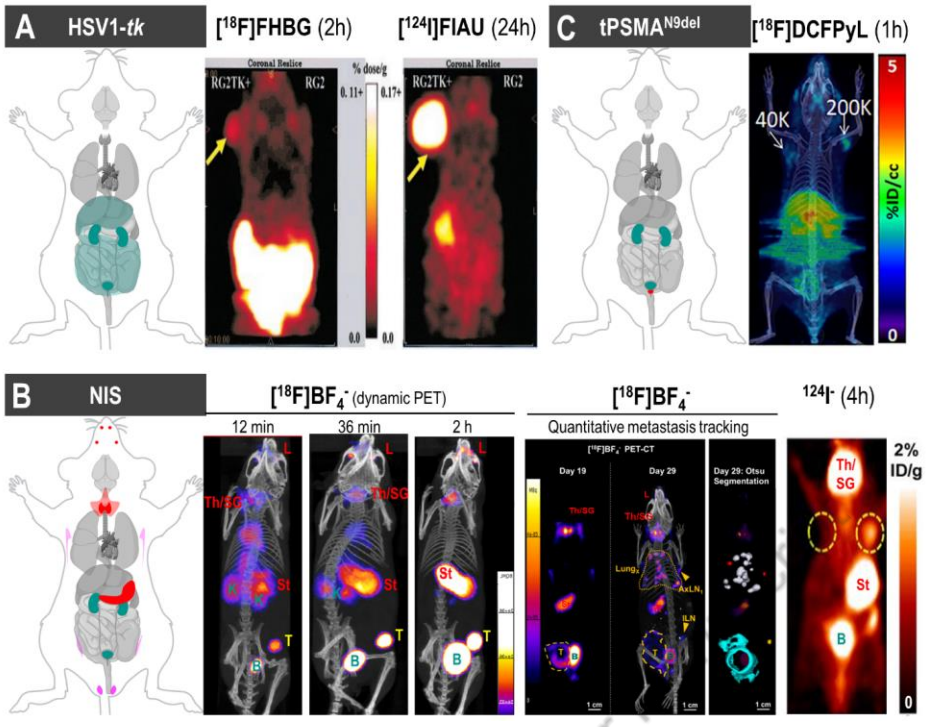

Figure 3. Background considerations for foreign and host radionuclide reporters | (A) HSV1-*tk* as an example of a foreign reporter is not expressed endogenously in healthy mammals. But this does not mean that the radiotracer to detect HSV1-*tk*-expressing cells is excluded from background uptake in other mammalian cells/organs or from generating signals during excretion (dark cyan in cartoon). Moreover, it is fundamental for radionuclide imaging that a contrast between background signal and signal arising from reporter-expressing cells (by one of the molecular imaging mechanisms (Fig.1C)) is generated through tissue clearance of radiotracer molecules. Radiotracers can thus affect background differently across different organs as shown here for two different PET radiotracers for HSV1-*tk*. Images are reproduced from a study comparing HSV1-*tk* radiotracer performance [151] with yellow arrows points towards the regions of interest in this study (tumours). Here, the other anatomical sites showing signals are of note (hepatobiliary and renal excretion for [^{18}F]FHBG and uptake into the stomach for [^{124}I]FAIU). **(B)** NIS is an example of a host reporter and consequently is expressed endogenously in some organs; NIS is highly expressed in the thyroid and stomach (red) precluding cell tracking from these organs and at low levels in testes (♂, pink), mammary (♀, pink), salivary and

lacrimal glands (light red). Images shown are from three different studies using varying PET radiotracers for NIS. **(*B/left*)** Images to the left demonstrate how [^{18}F]BF_4^- *in vivo* distribution changes over time (female mouse with mammary tumour indicated by a yellow "T"). For details see [46]. **(*B/middle*)** Images shown demonstrate metastasis tracking over time and exquisite resolution and sensitivity of NIS-PET imaging for metastasis tracking. They also demonstrate the necrotic tumour core, which is not imaged by NIS due to its favourable dependence on cellular energy for function, thereby reflecting cell viability. An example of Otsu image segmentation is shown to the right, which is the basis for quantitation (for details see [59]). Further annotations are endogenous signals from thyroid and salivary glands ("Th/SG"), stomach ("St") and lacrimal glands ("L"). **(*B/right*)** This image is reproduced from a study elucidating the detection sensitivity of reporter-expressing engineered primary T-cells [47] with annotations the same as in the left images. In both cases radiotracer excretion also leads to signals, in the case of these NIS tracers only from the renal excretion system ("K": kidneys, "B": bladder). **(C)** CAR-T cells were engineered to express the tPSMA^{N9del} reporter and administered to NSG mice at the indicated numbers (in 50μL 50% Matrigel; white arrows). Imaging with the radiotracer [^{18}F]DCFPyL resulted in CAR-T detection. Notably, images are not free of background despite PSMA endogenous expression limited to the prostate (red area in cartoon). This is because radiotracer clearance was incomplete at the point of imaging. To improve the display contrast of the *in vivo* images, the authors masked relatively high renal radiotracer uptake using a thresholding method. For experimental details see [29]. [All data images in this figure are reproduced with minor modifications from the publications mentioned in the legend, with permission from corresponding publishers].

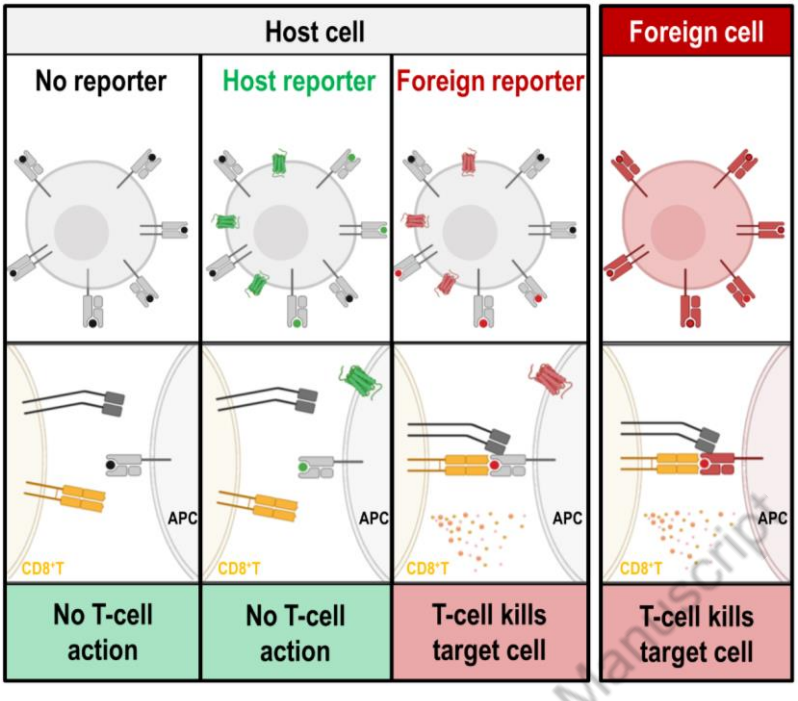

Figure 4. Recognition of reporter antigens by the immune system | The intact mammalian immune system operates several mechanisms to recognize cells expressing non-self (*i.e.* non-host) proteins. As one simplified example, we show here the recognition of antigen-presenting MHC class I molecules on antigen presenting cells (APC) by cytotoxic T-cells ($CD8^+T$). Host cells (far left column, black dots representing presented host antigens) are not recognised by $CD8^+T$ as they are pre-coded to not target self. In contrast, non-self MHC class I molecules on foreign cells (far right column) are recognised by $CD8^+T$, resulting in destruction of the foreign cells. If host cells express host reporters (centre left column, green), corresponding host antigens (green dots) can be presented on MHC class I molecules, and as they are representing self $CD8^+Ts$ take no action when they encounter these cells. If foreign reporters are expressed (centre right column), self MHC class I molecules present non-self/foreign antigens (red dots) resulting in $CD8^+T$ action and killing of the corresponding host cell due to the presence of the foreign reporter. The figure was generated using Biorender.com.

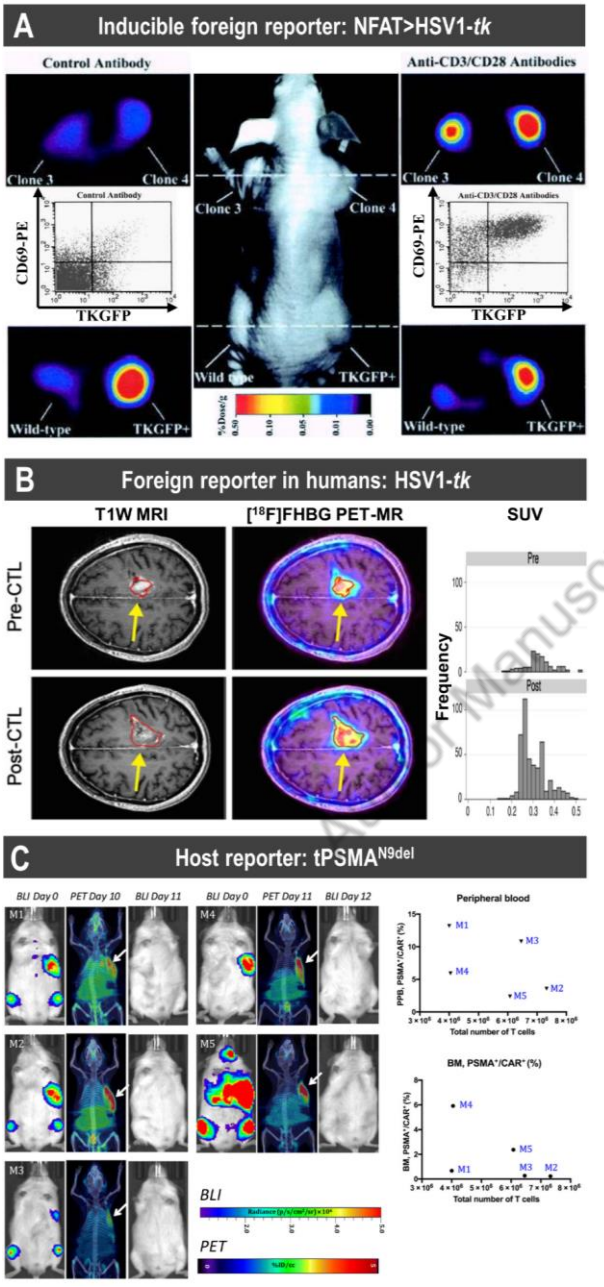

1461

Figure 5. Examples of foreign and host reporters for T-cell tracking. | (A) Proof-of-principle study demonstrating non-invasive imaging of T-cell activation by NFAT-driven expression of the reporters HSV1-*tk* and GFP (TKGFP) with [^{124}I]FIAU as a PET radiotracer for HSV1-*tk*. Photographic image of a typical mouse bearing different subcutaneous infiltrates **(*middle panel*)**; transaxial PET images of TKGFP expression in a mouse treated with control antibody **(*left panels*)** and T-cell activating anti-CD3/CD28 antibodies **(*right panels*)** were obtained at the levels indicated by the dashed lines of the middle panel. Samples are the Jurkat/dcmNFATtgn clones 3 and 4 (two similar clones), wild-type Jurkat infiltrates (no reporter control) and Jurkat/TKGFP (constitutive reporter expression as positive control). **(*Gray inset plots*)** FACS profiles for reporter expression (TKGFP) *versus* a T-cell activation marker (CD69) from a tissue sample obtained from the same Jurkat/dcmNFATtgn clone 4 infiltrate that was imaged with PET above. **(B)** [^{18}F]FHBG PET was performed in a 60-year-old male with multifocal left hemispheric glioma, who received cytotoxic T-lyumphocytes into the medial left frontal lobe tumour (yellow arrows). Tumour size was monitored by T1-weighted contrast-enhanced MRI **(*left panels*)**. [^{18}F]FHBG PET to detect HSV1-*tk* was recorded and images were fused with MR images **(*right panels*)**, and 3D volumes of interest were drawn using a 50% [^{18}F]FHBG SUVmax threshold, outlined in red. **(*Top row*)** Images and voxel-wise analysis of [^{18}F]FHBG total radioactivity prior to CTL infusion and **(*bottom row*)** one week after CTL infusion [76]. **(C)** Longitudinal imaging CAR-T tracking study demonstrating that the number of CD19-tPSMA^{N9del} CAR T-cells in the peripheral blood and the bone marrow does not correlate with the total number of the CD19-tPSMA^{N9del} CAR T-cells localised to the tumours. **(*Left*)** PET/CT and BLI images of five different mice. Days are marked from the day of CAR-T infusion. Mice were imaged on a SuperArgus small-animal PET/CT 1h after administration of 14.8 MBq [^{18}F]DCFPyL. Images alternate between fLuc-tagged bioluminescence (BLI, radiance) for visualisation of tumour cells and PET/CT for CAR T-cells, with each mouse undergoing both imaging studies. Arrows designate accumulation of CAR T-cells. To improve the display contrast of the *in vivo* images, the relatively high renal radiotracer uptake was masked using a thresholding method. Images are scaled to the same maximum value within each modality. **(*Right*)** Quantified numbers of the CD19-tPSMA^{N9del} CAR T-cells in the region of interest drawn to cover the entire tumour area were plotted with the percentage number of PSMA^{+}/CAR^{+} cell populations in the peripheral blood (PPB) and the bone marrow (BM). Each data point (M) represents each mouse. For details see [29]. [Figure modified from publications cited above with permissions obtained].

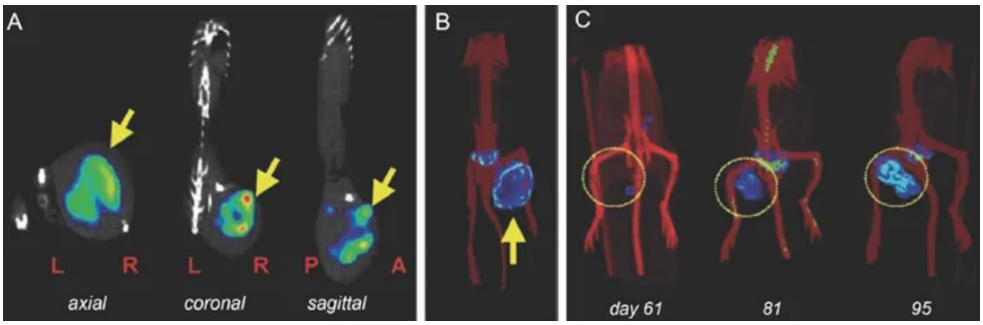

Figure 6. Example of reporter gene integration to enable non-invasive monitoring of stem cell mediated teratoma formation by *in vivo* imaging | Human ESCs were lentivirally modified to express the HSV1-*tk* radionuclide reporter gene fused to enhanced GFP and 2-5x10^6 reporter expressing hESCs were injected intramuscularly and tracked *in vivo* by whole-body SPECT/CT imaging. Yellow arrows/rings indicate tumours. Representative planar **(A)** γ and **(B)** SPECT/CT images of tumours derived in an animal scanned 87 days after tumour inoculation (when a palpable tumour was detected). The radiotracer [^{125}I]FIAU was i/v administered and the animal was scanned at 24h later. **(C)** Longitudinal SPECT/CT imaging of a different SCID-beige mouse harbouring a teratoma from reporter expressing hESCs. This mouse was serially imaged at the indicated time points post inoculation. All data were quantitatively analysed in this study. For details the reader is referred to the original work [123]. [Figure reproduced with minor modification from the cited work].

Table 1. Promising host-compatible reporter genes and their corresponding imaging tracers. | Promise was evaluated by the authors based on (i) human reporter origin ensuring no immunogenicity against the therapeutic cells expressing the reporter, and (ii) availability of at least one already clinically approved or first-in-man tried labelling agent.

Reporter				~~Contrast~~Imaging agent		Ref.
Class	**Name**	**Properties**	**AA***	**Modality**	**Properties**	
Transporter	Sodium iodide symporter (NIS, SLC5A5)	Symports Na^+ alongside various anions. Endogenous expression in thyroid, stomach, lacrimal, salivary and lactating mammary glands, small intestine, choroid plexus and testicles.	618	**PET:** $^{124}I^-$, $[^{18}F]BF_4^-$, $[^{18}F]SO_3F^-$, $[^{18}F]PF_6^-$. **SPECT:** $^{99m}TcO_4^-$, $^{123}I^-$.	Tracers do not cross blood brain barrier (BBB). Several tracers are clinically approved, most require no ($^{99m}TcO_4^-$, $^{xy}I^-$) or are made by automated synthesis [59].	[40-42, 152, 153]
	Norepinephrin transporter (NET, SLC6A2)	NaCl-dependent monoamine transporter. Endogenously expressed in organs with sympathetic innervation (heart, brain),	617	**PET:** [^{124}I]MIBG**; [^{11}C]hydroxyephedrine. **SPECT:** [^{123}I]MIBG**.	Tracers do not cross BBB.	[154]
	Dopamine transporter (DAT, SLC6A3)	NaCl-dependent.	620	**PET:** [^{11}C]CFT, [^{11}C]PE2I, [^{18}F]FP-CIT. **SPECT:** ^{123}I-β-CIT**, ^{123}I-FP-CIT**, ^{123}I-Ioflupane**, ^{99m}TRODAT.	Few data in public domain. Tracers cross BBB.	[155]
Enzyme	Pyruvate kinase M2	Expression during development, also in cancers.	531	**PET:** [^{18}F]DASA-23.	Background in organs of excretion route. Suggested for cell tracking within brain. Tracer crosses BBB.	[156]
	Thymidine kinase (hmtk2/hΔTK2)	Human kinase causing cellular tracer trapping.	265	**PET:** [^{124}I]FIAU**, [^{18}F]FEAU, [^{18}F]FMAU (for hTK2-N93D/L109F).	Tracers do not cross the BBB; Endogenous signals in gall bladder, intestine and organs involved in clearance.	[157]
	Deoxycytidine kinase (hdCK)	Human kinase causing cellular tracer trapping.	260	**PET:** [^{124}I]FIAU**, [^{18}F]FEAU.	Tracers do not cross the BBB; Endogenous signals in gall bladder, intestine and organs involved in clearance.	[32, 158]
Cell surface receptor	Somatostatin receptor type 2 (SSTR2)	G-protein-coupled receptor. Endogenous expression in brain, adrenal glands, kidneys, spleen, stomach and many tumours (*i.e.* SCLC, pituitary, endocrine, pancreatic, paraganglioma, medullary thyroid carcinoma, pheochromocytoma);	369	**PET:** ^{68}Ga-DOTATOC, ^{68}Ga-DOTATATE. **SPECT:** ^{111}In-DOTA-BASS. (best tracers selected here).	Tracers may cause cell signalling, change proliferation and might inhibit impair cell function. Non-metal octreotide radiotracers can cross BBB. Some tracers clinically approved. ^{68}Ga/^{111}In-based tracers are readily accessible.	[159-162]
	Dopamine receptor (D_2R)	G-protein-coupled receptor. High endogenous expression in pituitary gland and striatum.	443	**PET:** [^{18}F]FESP, [^{11}C]Raclopride, [^{11}C]N-methylspiperone.	Slow clearance of [^{18}F]FESP; Tracers cross BBB.	[163-166]
	Transferrin receptor (TfR)	Fast recycling receptor.	760	**MRI:** Transferrin-conjugated SPIO.	Transferrin-conjugated SPIO particles are internalised by cells.	[167]
Cell surface protein	Glutamate carboxy-peptidase 2 (PSMA) and variant $tPSMA^{N9Del}$	$tPSMA^{N9Del}$ has higher plasma membrane concentration. High expression in prostate.	750	**PET:** [^{18}F]DCFPyL, [^{18}F]DCFBC. **SPECT:** [^{125}I]DCFPyL**. Anti-PSMA antibodies and ligands can be flexibly labelled*, e.g J951-IR800.	Background signal in kidneys. Tracers do not cross BBB. Some tracers clinically approved.	[28, 29]
Cell surface-antigen	Human carcino-embryonic antigen-based reporters	CEA expressed in pancreatic, gastric, colorectal and medullary thyroid cancers. Reporters are recombinant proteins based on CEA minigene (N-A3) fused to extracellular and transmembrane	ca.460	**PET:** ^{124}I-anti-CEA scFv-Fc H310A**, [^{18}F]FB-T84.66 diabody	Tracers do not cross BBB. ^{99m}Tc-anti-CEA Fab' is clinically approved.	[103, 104, 168-170]

		domains of human FcγRIIb receptor, CD5 or TfR carboxyterminal domain.		**SPECT:** ^{99m}Tc-anti-CEA Fab', ^{111}In-ZCE-025, ^{111}In-anti-CEA F023C5i.[&]		
Artificial cell surface molecule	DOTA antibody reporter 1 (DAbR1)	scFv of murine anti-DOTA IgG1 antibody 2D12.5/G54C fused to human IgG4 CH2-CH3 and the transmembrane domain of human CD4.	ca. 470	**PET:** ^{86}Y-AABD.	^{86}Y-AABD is a DOTA complex that binds irreversibly to a cysteine of 2D12.5/G54C. Tracer does not cross BBB.	[101]
	Estrogen receptor α ligand binding domain (hERL)	No reported physiological function. Endogenous estrogen receptor expression limited to uterus, ovaries and mammary glands.	est[$] 250	**PET:** [^{18}F]FES.	Tracer is clinically used estrogen receptor imaging agent. ~~Contrast~~Imaging agent crosses BBB.	[30]
	Anti-PEG Fab fragment	Recombinant protein with N-terminal HA-tag, anti-PEG Fab followed by a c-myc epitope and eB7. Tags could cause immunogenicity.	812	**PET:** ^{124}I-PEG-SHPP**[,&]. **MRI:** SPIO-PEG. **Fluorescence:** *e.g.* NIR797-PEG.	Iodine tracers bear risk of deiodination. Some tracers cross BBB. PEG is non-toxic and approved by FDA.	[98]
Carrier protein	Ferritin	Human heavy and light chains co-expressed, or murine heavy chain only expressed as reporter.	Hu:183/175	**MRI:** iron.	Iron is not equally distributed across the brain and therefore may cause local susceptibility shifts that are above the MRI detection limit.	[171, 172]

* Amino acid chain length as an indication of reporter molecular weight (MW; not accounting for posttranslational modifications); wildtype reporter MWs are indicated.

** Radioiodinated tracers can become de-iodinated *in vivo* resulting in free iodide that is subsequently taken up into NIS expressing organs (see table above).

[&] Any other modality can be used provided a suitable contrast forming moiety will be attached to PEG and the CEA antibodies, respectively.

[$] Report [30] does not clearly describe reporter construction leaving precise reporter size only to be estimated; we estimate it based on the estrogen receptor α ligand binding domain, which is approx. 250 amino acids long (*cf.* http://pfam.xfam.org/family/PF02159).

Table 2 Non-mammalian reporter genes and their corresponding imaging tracers.

Reporter				~~Contrast~~Imaging Agent		Ref
Class	**Name**	**Properties**	**AA***	**Modality**	**Properties**	
Enzyme	β-galactosidase	Glycoside hydrolase enzyme; product of LacZ gene and isolated from *E. coli*	1021	**OPTICAL CL:** Near-Infrared Dioxetane Luminophores (emission λ = 690 nm) **MRI:** EgadMe&. **PET**: 2-(4-[^{123}I]iodophenyl)ethyl-1-thio-β-D-galactopyranoside, 3-(2'-[^{18}F]fluoroethoxy)-2-nitrophenyl-β-D-galactopyranoside, 3-[^{11}C]methoxy-2-nitrophenyl-β-D-galactopyranoside; [^{18}F]FPyGal **SPECT:** 5-[^{125}I]iodoindol-3-yl-β-D-galactopyranoside ([^{125}I]IBDG); 4-chloro-3-bromoindole-galactose (X-gal);	Cellular toxicity depending on the substrates; lack of sensitivity and high background; rapid renal clearance of ([^{125}I]IBDG) impedes intratumoral availability if systemically administered	[173-179]
	E. coli dihydrofolate reductase (eDHFR)	Catalyses NADPH-dependant reduction of folate; inhibited by highly specific small molecule trimethoprim	159	**PET:** [^{11}C]Trimethoprim; [^{18}F]-trimethoprim (TMP)	Rapid renal clearance and hepatobiliary metabolism	[180, 181]
	HSV1-*tk* and mutants	Kinase causing cellular tracer	376	**PET:** [^{124}I]FIAU, [^{18}F]FEAU, [^{18}F]FHBG.	Tracers do not cross blood-brain barrier.	[182-186]
	Emerald luciferase (ELuc) and mutants	Catalyses oxygenation of D-luciferin to oxyluciferin ; emits strongest luminescence among beetle luciferases; from click beetle *Pyrearinus termitilluminans*	543	**OPTICAL BL:** D-luciferin/ATP (emission λ=534-626 nm; depending on WT/mutant used)	Lack of signal in the brain as the substrate cannot cross BB barrier; low thermostability and low light intensity	[187-190]
	Firefly luciferase (Fluc) and mutants	Catalyses the oxygenation of d-luciferin to oxyluciferin; derived from the North American firefly (*Photinus pyralis*)	550	**OPTICAL BL:** D-luciferin/ATP (emission λ=550–615 nm; depending on WT/mutant used)	Depending on the type used: high thermolability and exhibits a bathochromic shift at >30°C and pH levels <7.8	[191-193]
	Gaussia luciferase (Gluc) and mutants	From *Gaussia princeps;* one of the smallest luciferases cloned so far; catalyses the oxidative decarboxylation of coelenterazine to produce luminescence	185	**OPTICAL BL**: Coelenterazine (emission λ=480-513 nm; depending on WT/mutant used)	No clinical use; background auto-luminescence	[194-197]
	Green Click Beetle luciferase and mutants	Derived from *Pyrophorus plagiophthalamus*	542	**OPTICAL BL**: Luciferin (emission λ=543)	No clinical use	[198]
	NanoLuc	Derived from *Oplophorus gracilorostris* (deep sea shrimp)	171	**OPTICAL BL**: Imidazopyrazinone substrate (furimazine) (emission λ=456nm)	Signal is heavily attenuated in tissues	[199-202]
	Renilla luciferase (RLuc) and mutants	Derived from *Renilla reniformis* (Sea Pansy)	311	**OPTICAL BL**: Coelenterazine (emission λ=475-535 nm; depending variant)	WT RLuc suffers from low stability in serum and thermolability at >30°C	[192, 203, 204]

Transporter	MS-1 *magA*	Putative ion transport protein from magnetotatic bacteria (*magnetopsinillum sp.strain AMB-1*)	434	**MRI:** Endogenous or exogenous Fe	Delay of change in signal, that is dependent on Fe availability	[205-207]
	Sodium-Taurocholate Cotransporting Polypeptide (NTCP)		349	**MRI:** Indocyanine green (ICG)		[208]
Artificial protein	Lysine-rich protein	Frequency-selective contrast, based on transfer of radiofrequency labeling from the reporter's amide protons to water protons	200	**MRI:** chemical exchange saturation transfer (CEST) MR imaging		[209, 210]
Fluorescent Proteins	mNeptune	fluorescent protein chromophore; derived from *Entacmaea quadricolor*	244	**OPTICAL FL**: (emission λ=650nm)	No clinical use	[211]
	mPlum	fluorescent protein chromophore; derived from DsRed of *Discosoma* (sea anemone)	226	**OPTICAL FL**: (emission λ=649nm)	No clinical use; low acid sensitivity	[212]
	mTagRFP	fluorescent protein chromophore; derived from *Entacmaea quadricolor*	238	**OPTICAL FL**: (emission λ=584nm)	No clinical use	[213]
	E2-Crimson	Derived from Ds-Red-Express2	225	**OPTICAL FL**: (emission λ=543nm)	No clinical use	[214, 215]
NIR fluorescent protein	iFP1.4	Requires exogenously added biliverdin as a co-factor; derived from *Deinococcus radiodurans*	328	**OPTICAL FL**: (emission λ=708nm)	No clinical use	[216, 217]
	iRFP 670	Endogenous biliverdin sufficient as a co-factor; derived from *Rhodopseudomonas palustris CGA009*	312	**OPTICAL FL**: (emission λ=670nm)	No clinical use	[216, 218, 219]
	iRFP 713	Endogenous biliverdin sufficient as a co-factor; derived from *Rhodopseudomonas palustris*	317	**OPTICAL FL**: (emission λ=713nm)	No clinical use	[216, 218-220]
	iRFP 720	Endogenous biliverdin sufficient as a co-factor; derived from *Rhodopseudomonas palustris*	317	**OPTICAL FL**: (emission λ = 720nm)	No clinical use	[221, 222]
Gas-filled protein complex	Gas vesicle structural protein A / Gas vesicle protein C	Gas vesicles generate contrast; gas vesicles occupy more than 10% of the volume of transduced cells GvpA; derived from *Dolichospermum lemmermannii*; GvpC; derived from *Dolichospermum flosaquae*	GvpA: 71 GvpC: 193	**Ultrasound**: 2.7-4.7 MPa insonation		[223, 224]
	Mammalian acoustic reporter gene (mARG)	Gas vesicles generate contrast ;	2500	**Ultrasound**: 3.2 MPa insonation		[224]

* Amino acid chain length as an indication of reporter molecular weight (MW; not accounting for posttranslational modifications); wildtype reporter MWs are indicated.

[&]EgadMe = 1-(2-(β-galactopyranosyloxy)propyl)-4,7,10tris(carboxymethyl)-1,4,7,10-tetraazacyclododecane)gadolinium(III).

Abbreviations: CL = Chemiluminescence; BL = Bioluminescence; FL = fluorescence imaging.

Table 3. Preclinical studies utilising reporter gene tracking of stem cell therapies.

Table illustrating the range of preclinical stem cell therapy studies that have incorporated reporter gene-afforded *in vivo* imaging. Studies are classified based on type of stem cell, with details on the modality and purpose of *in vivo* tracking used as well as the reporter gene and method of construct integration.

Cell therapy	Purpose of imaging	Reporter gene (RG) expressed	Imaging modality used	Method of RG transfer	Ref
Adult stem cells/tissue resident stem cells					
Human and mouse HSCs	Engraftment monitoring	human deoxycytidine kinase with 3 amino acid substitutions within the active site (hdCK3mut)	PET/CT	Lentivirus	[225]
Immortalised human neural stem cell line (HB1.F3)	Study of epigenetic silencing mechanisms of reporter genes in neural stem cells	hNIS	Scintographic imaging	Plasmid transfection	[226]
Immortalised human bone marrow derived MSC line	Monitoring of MSC homing to tumours and evaluation of their therapeutic potential as a transgenic reporter expressing cell-based therapy	hNIS	Scintographic imaging	Plasmid transfection	[227]
Human MSCs	Monitoring of MSC homing and therapeutic potential in breast cancer	hNIS	SPECT	Adenovirus	[228]
Human MSCs	Tracking of long-term fate and trafficking of MSCs	Triple fusion protein: fLuc-mRFP-HSV1-sr39tk	BLI and PET/CT	Lentivirus	[229]
Human MSCs	Understanding MSC fate in tissue repair	Mutant of dopamine type 2 receptor (D2R80A)	PET	Lentivirus	[230]
Human MSCs	Evaluating myocardial tracking potential with a PET reporter in small (rat) and large animal studies (swine)	HSV1-sr39tk	PET	Adenovirus	[125]
hESCs and their differentiated progeny					
Transplanted labelled hESCs/H9 line	Tracking immune rejection	Fusion protein: fLuc and eGFP	BLI	Lentivirus	[231]
Human neural stem cells derived from hESCs/H7 line	Tracking fate and function of grafted cells in a preclinical stroke model	Triple fusion protein: mRFP-fLuc-HSV1-sr39tk	MRI and PET	Lentivirus	[232]
hESCs	Teratoma monitoring after transplant into chick embryos and mice (kidney capsule and muscle of peritoneum)	fLuc	BLI	Plasmid transfection	[233]
Human ESCs/H9 line	Determining application of genome editing for long-term molecular imaging of engrafted stem cells	Polycistronic: eGFP/fLuc/hSSTR2 and polycistronic eGFP/fLuc/hNIS	BLI and PET	ZFN targeted at the AAVS1 locus	[234]

hESCs/H9 line and one patient derived hiPSC line and hESC-derived ECs and CMs	Preclinical monitoring of teratomas and hESC-derived cardiac cells for cardiovascular research/regenerative medicine	Triple fusion protein: fLuc-mRFP- HSV1-*tk*	BLI	ZFN targeted at the AAVS1 locus	[235]
hESC-derived CD34$^+$ cells/H9 line	Tracking engraftment/ developmental of hESC-derived HSCs *in vivo*	fLuc	BLI	Transfection of DNA transposon system	[236]
hESCs/H9 line	Safety study: analysis number of contaminating undifferentiated hESCs required to yield a teratoma	Fusion protein: fLuc-eGFP	BLI	Lentivirus	[122]
hESC-derived MSCs	Studied the distribution of human MSCs in a rat hind limb ischemic injury model immediately after transplantation and also analysed the recipient tissue response to transplanted cells	fLuc	BLI	Lentivirus	[237]
hESCs and hESC-derived ECs/H9 line	Comparison of MR & bioluminescence modalities for tracking of transplanted cell engraftment and longitudinal monitoring of cell fate	fusion protein: fLuc-eGFP	BLI	Lentivirus	[238]
hESC-derived neural precursors/H9 line	Monitoring of long-term viability and proliferation of hESC-derived neural precursor grafts in the brains of immunodeficient and immunocompetent mice.	TGL fusion protein: HSV1-*tk*-eGFP-fLuc	BLI	Lentivirus	[239]
hESC-derived skeletal myoblasts/H1 and H9 lines	Assessment of long-term myoblast engraftment and survival with monitoring for teratoma formation	TGL fusion protein: HSV1-*tk*-eGFP-fLuc	BLI	Lentivirus	[240]
hESCs/H1 and H9	Monitoring stem cell engraftment and teratoma formation	Bicistronic fLuc and GFP and fusion of HSV1-*tk*-GFP	BLI and SPECT/CT	Lentivirus	[241]
hiPSCs and their differentiated progeny					
hiPSCs differentiated to motor neurons, HLCs and macrophages	Generation of reporter expressing hiPSCs suitable for differentiation into macrophages to track anti-fibrotic potential *in vivo*	Zsgreen	*In vivo* imaging not performed*	ZFN targeted at AAVS1 locus	[242]
hiPSC-derived HLCs	Potential for tracking transplanted HLC populations *in vivo*	hNIS-eGFP fusion	SPECT/CT	Lentivirus	[243]
hiPSC-derived neural stem/progenitor cells	Determining the feasibility of tumour ablation following hiPSC-NS/PC spinal cord transplantation utilising immunoregulation	Fusion protein Venus-fLuc	BLI	Lentivirus	[244]
hiPSC-derived endothelial cells	Analysis of potential of iPSC-derived ECs to promote perfusion of ischaemic tissue in model of peripheral arterial disease	Fusion protein: fLuc-eGFP	BLI	Lentivirus	[245]
hiPSCs	Evaluation of transplanted hiPSC survival, engraftment, and distribution of in a pig model of myocardial infarction	Bicistronic ratNIS and Venus	SPECT/CT	Plasmid transfection	[246]

hiPSCs	evaluating systems to purge residual hiPSCs before graft without compromising hematopoietic repopulation capability	fLuc	BLI	Lentivirus	[247]
hiPSC-derived cardiomyocytes	Assessment of relationship between transplanted cell number and engraftment rate in myocardial injury	Bicistronic fLuc and GFP	BLI	Lentivirus	[248]

Abbreviations: HSC= haematopoietic stem cell, hESC = human embryonic stem cell, hiPSC = human induced pluripotent stem cell, RG = reporter gene, ECs = Endothelial cells, CMs = Cardiomyocytes, HLCs = hepatocyte-like-cells, ZF = Zinc finger nuclease, fLuc = Firefly Luciferase, mRFP = monomeric red fluorescence protein, HSV1-*tk* = herpes simplex virus type 1 thymidine kinase, HSV1-sr39tk = truncated HSV1-sr39 thymidine kinase, hNIS = human sodium iodide symporter, hSSTR2 = human somatostatin receptor 2, BLI = bioluminescence imaging.
*cited as a tool with the potential for macrophage *in vivo* tracking in future.

***** End of Manuscript *****